Research article

Geoenergy

https://doi.org/10.1144/geoenergy2023-008 | Vol. 1 | 2023 | geoenergy2023-008

Late Permian evaporite facies variation in the Forth Approaches Basin, North Sea: implications for hydrogen storage

Rachel E. Brackenridge*, Lauren J. Russell, Adrian J. Hartley, Douglas Watson and Thomas Houghton

School of Geosciences, University of Aberdeen, Meston Building King's College, Aberdeen AB24 3UE, UK
REB, 0000-0002-0572-314X
* Correspondence: rachel.brackenridge@abdn.ac.uk

Abstract: Hydrogen is expected to play a key role in decarbonizing industry and storing energy from intermittent sources such as wind energy. Underground salt caverns are an attractive target for storage due to their large volumes and effective sealing capacity. Despite ambitious goals to become a world leader in hydrogen, there are no onshore salt basins in Scotland. Therefore, the offshore Forth Approaches Basin (FAB), currently undergoing development of the Seagreen Offshore Wind Farm, could provide a critical storage site. Re-evaluation of petrophysical data from five legacy hydrocarbon wells allowed an updated assessment of the composition and variability of the Late Permian Zechstein evaporite sequence. Well analysis is combined with seismic interpretation to understand the salt bodies and their suitability for solution mining. Three halite formations are identified: (1) the Stassfurt Halite Formation, which has insufficient thickness for solution mining; (2) the Leine Halite Formation, which comprises three subunits with a KCl-dominated unit separating two halite-dominated units; and (3) the Aller Halite Formation, which is only identified in the centre of the FAB. Where halokinesis has occurred, the Leine Halite Formation reaches sufficient thicknesses (>300 m) and purity for salt cavern placement; however, heterogeneities are challenging to predict. Layered evaporites only reach sufficient thickness where the Aller Halite Formation is present and could be developed with the underlying Leine Halite Formation. Heterogeneities can be correlated across wells within the layered sequences, aiding prediction. A strong understanding of evaporite facies distribution is required to ensure that halite bodies are suitable for safe and economic solution mining in the FAB and other salt basins globally.

Thematic collection: This article is part of the Hydrogen as a future energy source collection available at: https://www.lyellcollection.org/topic/collections/hydrogen

Received 21 February 2023; **revised** 3 May 2023; **accepted** 11 May 2023

In line with ambitious net zero targets, the UK is stepping up its hydrogen capability with future opportunities for use in the decarbonization of transport, heating and power generation (HM Government 2021). Hydrogen provides a low-carbon energy source that can be produced from renewable sources (wind, solar and tidal) through electrolysis or, when combined with carbon capture and storage (CCS), through steam methane reforming from natural gas (Stephenson *et al.* 2019). Subsurface hydrogen storage enables large quantities of energy to be stored to facilitate the intermittency of renewable power sources and fluctuating energy demand (Crotogino *et al.* 2010; Gahleitner 2013; Tarkowski 2019).

Proximity to energy sources and infrastructure plays a key role in the economic feasibility of a storage site (Tarkowski 2019), and subsurface geology is a critical control. Hydrogen storage in porous rocks such as depleted oil and natural gas fields and aquifers, as well as within disused mine workings, are currently under research (Heinemann *et al.* 2018; Lysyy *et al.* 2021; Franklin *et al.* 2022). The use of solution mining of salt caverns provides an attractive alternative owing to halite's strong sealing properties, low working/cushion gas ratios, high potential injectivity rates and capacity for high annual turnover frequencies compared to depleted hydrocarbon fields or aquifers (Crotogino 2022). The applicability and long-term safety of hydrogen storage within salt caverns is proven (Tarkowski 2019; Duffy *et al.* 2022; Williams *et al.* 2022), with active onshore storage sites occurring within layered evaporites at Teeside, UK since 1972 (Beutel and Black 2005; Stone *et al.* 2009) and more recently within salt domes at three sites in the USA: Clemens, Moss Bluff and Spindletop (Kruck *et al.* 2013; Duffy *et al.* 2022). This is a sector that is seeing active investment and development (e.g. the HyCAVmobil project, Germany: Sarajlic *et al.* 2021). Salt caverns have also been used for the intermittent storage of gas and compressed air, demonstrating that solution mining of salt for storage can be safe and economic with a low environmental impact (Crotogino *et al.* 2010). In the UK, salt cavern natural gas stores can be found within Permian and Triassic halites in Yorkshire and Cheshire (Evans and Holloway 2009).

In Scotland, there are no onshore salt basins that could provide local storage for industrial centres in the Midland Valley or NE Scotland (Fig. 1), limiting the possibility of onshore subsurface hydrogen storage to porous rocks and man-made alternatives (Heinemann *et al.* 2018; Franklin *et al.* 2022). However, recent advances in processing and infrastructure facilities are allowing the development of offshore hydrogen production that can link directly with offshore wind farms for the first time (Caglayan *et al.* 2020; Baraniuk 2021; Tractebel Engie 2021), with the possibility of technologies being in place by 2025 (Baraniuk 2021). This would be an important step to making offshore salt cavern storage viable and economic, particularly where salt basins exist in the subsurface close to offshore wind farms. The Forth Approaches Basin (FAB) is currently undergoing the development of the extensive Seagreen offshore wind farm (Seagreen Wind Energy 2014). This, combined with its favourable geology, mean that it could provide an alternative storage site to meet the hydrogen storage needs of Scotland.

For a site to be geologically suitable for salt cavern storage, the targeted halite store must fulfil a number of criteria. The halite bed(s) should be sufficiently thick to allow an economic cavern volume with adequate roof and floor thicknesses to ensure structural integrity (Williams *et al.* 2022). They should be buried to a depth

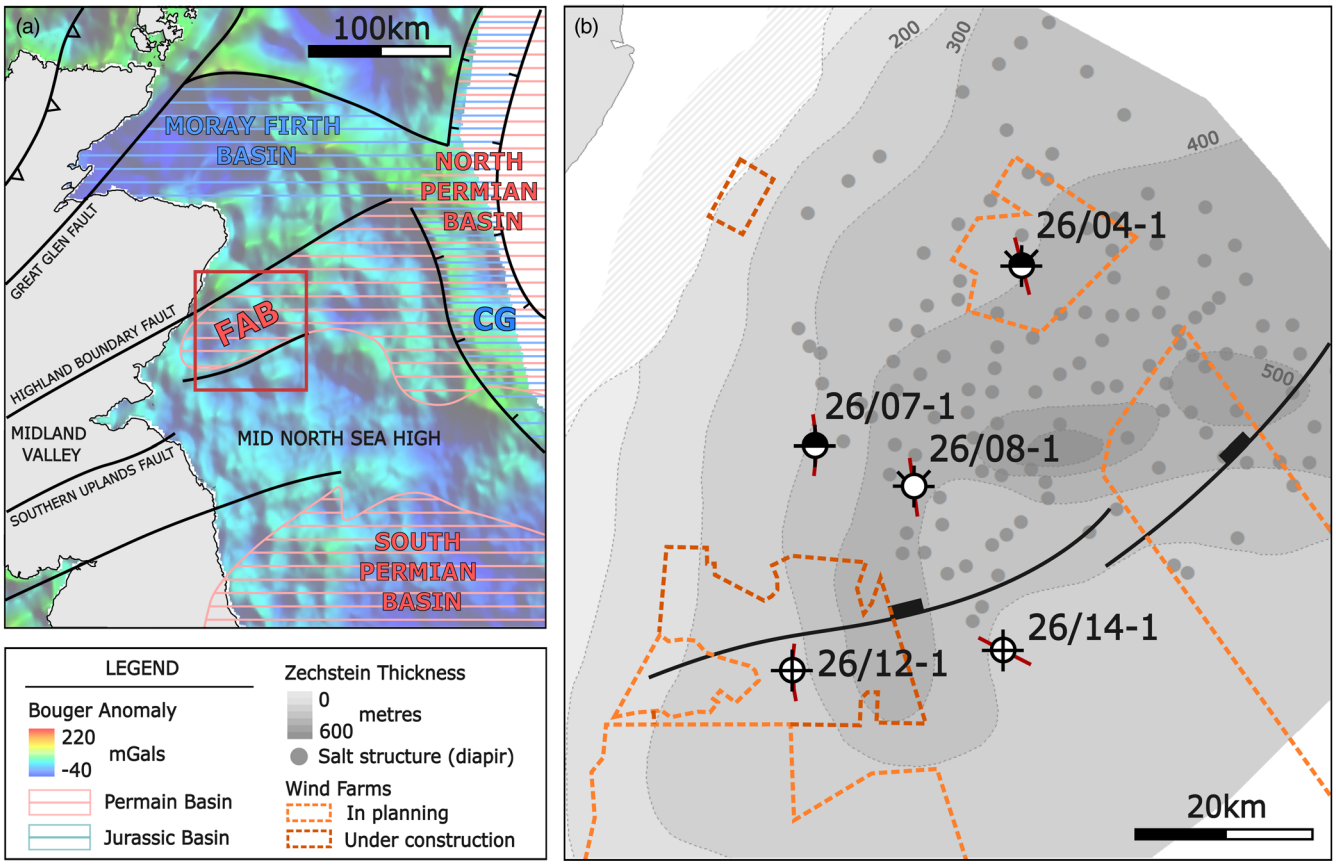

Fig. 1. (**a**) Regional map of the UK North Sea with key structural features and onshore salt storage sites. The location of the Forth Approaches Basin (FAB) is highlighted in red. CG, Central Graben. (**b**) Salt distribution in the FAB with the data used in this study (from Cartwright *et al.* 2001). Planned offshore wind farms indicated. Fault is Carboniferous in age (from Cartwright *et al.* 2001).

that provides an optimal pressure regime – deep enough to avoid gas outbursts but not so deep as to allow pressure-induced salt creep (Smith *et al.* 2005; Tarkowski 2019). Halite purity is a key consideration when assessing a potential salt cavern site (Duffy *et al.* 2022). Intra-salt heterogeneities can impact well and cavern integrity (Warren 2017). Heterogeneities within halite layers such as carbonate and clastic units or other salts can react with injected fluids and control the geometry and stability of the salt cavern (Duffy *et al.* 2022). It is therefore vital to understand the internal structuration of salt bodies, particularly where deformation has occurred (e.g. within salt diapirs).

This research aims to assess the geological adequacy of the Late Permian Zechstein evaporite sequence for hydrogen storage in the FAB. This will be done through: (1) assessing the depth and thickness of halite layers identified at well sites in the FAB; (2) reviewing facies variability within the Zechstein succession; and (3) using seismic data to understand the degree of halokinesis at each well site and its control on facies heterogeneity. Understanding the geological limitations and opportunities of the FAB for subsurface storage could help to support the expanding hydrogen economy in the NE of Scotland (Element Energy 2020) and provide learnings in regions where a move to a hydrogen economy is favourable (Bossel and Eliasson 2003). This study also provides an opportunity to assess the re-purposing of data acquired for the hydrocarbon industry for low-carbon energy purposes.

Geological setting

The FAB is a NE–SW-trending basin located 50 km SE of Aberdeen, and resides between the Highland Boundary Fault to the north and Southern Upland Fault Zone to the south (Cartwright *et al.* 2001; Arsenikos *et al.* 2019) (Fig. 1). Following Early–Mid Devonian post-orogenic Caledonian collapse, Upper Devonian fluvial sandstones sourced proximally from north of the Highland Boundary Fault accumulated across the FAB (Arsenikos *et al.* 2019; McKellar *et al.* 2020). Extension in the Early Carboniferous resulted in the development of a major SW–NE-trending half-graben into which a thick synkinematic accumulation of Carboniferous fluvio-deltaic facies accumulated in the hanging wall (Glennie and Underhill 1998; Cartwright *et al.* 2001; Kearsey *et al.* 2019). In the Late Carboniferous (Westphalian), extension ceased and compressional movements associated with the Variscan Orogeny resulted in non-deposition and erosion across the basin (Glennie and Underhill 1998; Cartwright *et al.* 2001). Above the resultant Base Permian Unconformity, Permian Rotliegend sands are observed in two wells within the basin and show thickening towards the basin-bounding fault (Fig. 1).

Continued post-Variscan orogenic collapse and thermal subsidence through the Late Permian resulted in a major marine transgression across the region that initiated the deposition of the Zechstein Group (Clark *et al.* 1998; Cartwright *et al.* 2001; Doornenbal and Stevenson 2010). The Zechstein Group extends across the Forth Approaches, North Permian and South Permian basins where it has been characterized and divided into five carbonate–evaporite cycles that were controlled by changes in eustatic sea level and extensional tectonics (Tucker 1991) (Fig. 2). Decreases in sea level resulted in this inland sea becoming disconnected from the world ocean. This disconnect coupled with minimal precipitation and marine incursions resulted in basinal waters frequently becoming increasingly saline (Tucker 1991). Evaporation of the salty brines facilitated the precipitation of thick evaporite sequences. Sea-level rise increased water depth within the basin and re-established a marine connection, allowing for the deposition of extensive carbonate sequences and mudstones. The

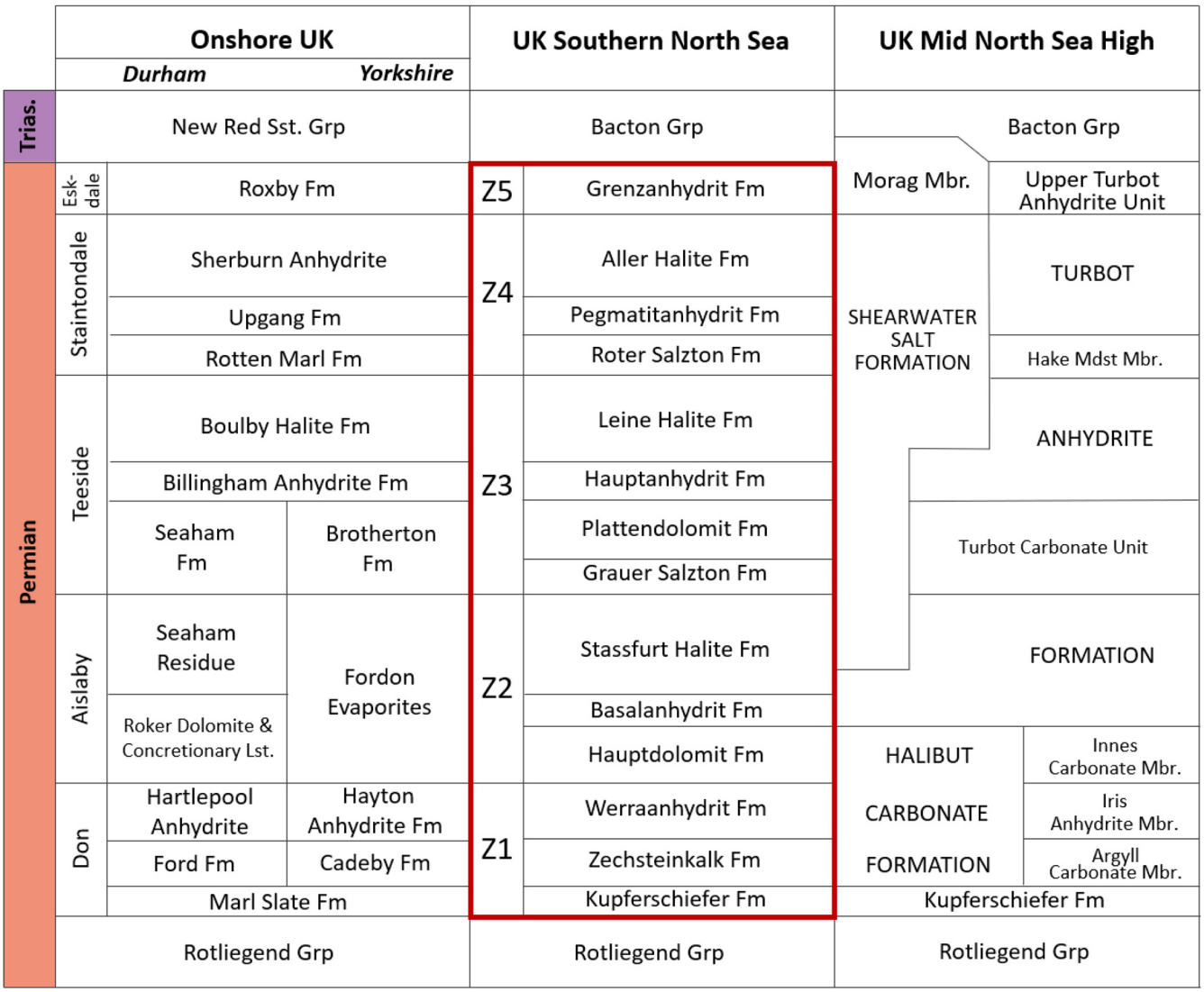

Fig. 2. Correlation and nomenclature of the Zechstein Group across the North Sea Region. The red box highlights the nomenclature used in this study. Sources: onshore UK nomenclature from Evans and Holloway (2009); UK Southern North Sea nomenclature from Johnson *et al.* (1993); UK Mid North Sea High nomenclature from Cameron (1993).

thickness of halite sequences and their presence overlying carbonate platforms suggests that precipitation continued until highstand conditions (Van den Belt and De Boer 2014). Subsequent incursions, evaporation and sea-level rise allowed the repetition of this depositional cycle. Five such cycles constitute the Zechstein Group (Smith 1989), although their distribution is variable across the North and South Permian basins (Fig. 2) as it is controlled by palaeotopography and basin connectivity (Cameron 1993; Johnson *et al.* 1993; Van Adrichem-Boogaert and Kouwe 1994).

Marine regression in the Late Permian–Early Triassic (Goldsmith *et al.* 1995; Fisher and Mudge 1990) marked the end of evaporite precipitation and the onset of Late Permian–Triassic terrestrial deposition. Extension across the North Sea region occurred in the Early Triassic but the exact timing and extent is difficult to constrain due to its thin-skinned nature and subsequent halokinesis (Erratt *et al.* 1999). Sedimentation in the FAB during the Triassic was controlled by salt mobility, where accommodation space is quickly filled, which leads to sedimentary loading and further halokinesis (Cartwright *et al.* 2001). The Base Cretaceous Unconformity overlies the Triassic succession, as calibrated from nearby well 27/03-1 (Cartwright *et al.* 2001). During the Late Jurassic–Early Cretaceous a major episode of extension occurred to the east of the FAB to form the trilete rift system of the Viking Graben, Moray Firth Basin and the Central Graben (Erratt *et al.* 1999) (Fig. 1). Later uplift to the west of the FAB (possibly related to the opening of the proto-Atlantic Ocean) resulted in erosion of stratigraphy at the seabed along its western margin (Brackenridge *et al.* 2020).

Exploration history

Exploration well 26/14-1 was the first to be drilled in the basin in 1984 (Table 1). This wildcat well targeted a base Zechstein structural high in the south of the FAB seeking Permian Rotliegend Leman sandstones (Neville and Wreglesworth 1984). The Z3 Plattendolomit Formation and Devono-Carboniferous sandstones were secondary targets. A good set of data was collected, including a full suite of logs (Table 2). Sedimentological core analysis concluded that a thin (8.5 m) Rotliegend overlies Devonian Old Red Sandstones (Gearhart Geodata Services 1984). However, the biostratigraphy report highlighted that the section was barren and did not show the characteristic red colouring of the Rotliegend elsewhere in the North Sea (Neville and Wreglesworth 1984), suggesting that the Rotliegend may be absent from this palaeohigh. No shows were identified.

This failed exploration well was closely followed by two more wells. First, well 26/07-1 located on the western margin of the FAB

Table 1. *Hydrocarbon exploration wells in the Forth Approaches Basin (FAB)*

Well	Completion date	Primary objective	Secondary objective	Hydrocarbons
26/14-1	June 1984	Permian Rotliegend	Zechstein, Carboniferous, Devonian	Dry
26/07-1	May 1985	Permian Rotliegend, Carboniferous	Triassic	Oil show, Zechstein
26/12-1	November 1986	Permian Rotliegend, Carboniferous, Devonian		Dry
26/08-1	November 1992	Lower Carboniferous		Weak gas shows, Lower Carboniferous
26/04-1	November 2001	Permian Rotliegend	Zechstein	Oil and gas shows, Zechstein

(Fig. 1; Table 1). Pre-Zechstein sandstones within large pinchout traps were the primary targets, with Triassic sandstone in a shallow four-way dip structure a secondary target (Wiggin 1985). A 152 m net Rotliegend sandstone was encountered, and the well penetrated a further 910 m of heterolytic Carboniferous section. All sands were water-bearing. No Triassic reservoir was identified (Wiggin 1985). A full suite of logs were collected below the 13⅜ inch casing shoe at 985.5 m measured depth (MD). An oil show was recorded in the Z2 Hauptdolomit Formation (Wiggin 1985); however, no well tests were completed.

The following year, well 26/12-1 was spudded (Table 1) just 21.5 km west of 26/14-1 on the eastern margin of the FAB (Fig. 1). The well targeted pre-Zechstein sands on a structural high, similar to that observed at well 26/14-1 (Cluff Oil 1986). However, both the Rotliegend and Carboniferous were absent, and altered Devonian sandstones were encountered directly below the Zechstein. No potential reservoir sections were identified and no hydrocarbons were recorded (Cluff Oil 1986). Despite this, a good suite of wireline logs were collected from a casing shoe at 367 m MD (Table 2).

Well 26/08-1 spudded in 1992 in the centre of the basin, aiming to test Lower Carboniferous fluvio-deltaic sandstones within a pre-Zechstein fault-bounded structure (Mobil North Sea 1993) (Fig. 1; Table 1). The targeted Lower Carboniferous (Visean) sands were significantly deeper than prognosed, and reservoir quality was poor as a result. Weak gas shows were recorded throughout the Lower Carboniferous but the lacustrine source rock was deemed at an earlier stage of maturation than prognosed, and intraformational seals were ineffective. A good suite of wireline logs were collected from a casing shoe close to the base of the Triassic at 769 m MD.

Following a hiatus in drilling activity, 26/04-1 was the final well to be drilled in 2001 (Glenister *et al.* 2002). The primary target Rotliegend sandstone was absent, with the Devonian sitting directly below the Zechstein. A mounded feature within the Zechstein, interpreted to be a reefal mound, showed thin reservoir sections in the Z3 Plattendolomit Formation and the Z2 Hauptdolomit Formation. Significant shows are recorded in the Plattendolomit Formation (64% hydrocarbon saturation), possibly sourced from the Permian Kupfershiefer; however, the accumulation was deemed uneconomic (Glenister *et al.* 2002). A good set of logs were collected from the Plattendolomit Formation at 945 m MD (Table 2).

Despite promising indications of a working petroleum system and multiple reservoir targets, no further wells have been drilled in the basin. The basin is now undergoing development of numerous offshore wind farms (Fig. 1).

Data and methods

Data from the five hydrocarbon exploration wells drilled within the FAB are the key dataset used in this study (Fig. 1; Table 1). Well logs and reports for these wells were obtained from the UK North Sea Transition Authority (NSTA) National Data Repository. The study of well data was primarily used to: (1) define formation boundaries and thicknesses; (2) correlate lithostratigraphic and chronostratigraphic packages across the basin; and (3) distinguish heterogeneities and quantify the abundance of impurities within the evaporite sequence.

Initial formation boundaries were taken from well reports. All well reports use the UK Southern North Sea nomenclature as described by Johnson *et al.* (1993) (Fig. 2). Petrophysical data availability varied between wells (Table 2). However, gamma ray (GR) logs were available for all, with other log availability more variable over the Zechstein section (Table 2). Well 26/14-1 has a full suite of logs available over the section of interest. This well also has an additional biostratigraphy study available (Neville and Wreglesworth 1984), which adds confidence to the facies and well top interpretation. As a result, well 26/14-1 was used to characterize the log responses of the Zechstein facies in this study. This log suite was used to conduct petrophysical analysis of the Zechstein facies where data quality and availability allowed. Log responses were cross-checked with mud logs and geological end of well reports (Neville and Wreglesworth 1984; Wiggin 1985; Cluff Oil 1986; Mobil North Sea 1993; Glenister *et al.* 2002) to make a revised interpretation of the Zechstein facies in the FAB, and formation tops were revised where necessary. All analysis was completed in Schulmberger's Petrel software. Results were cross-checked against published examples of the petrophysical response of the Zechstein and other evaporitic sequences (Fig. 3; Table 3) (Evans and Holloway 2009; Crain 2014; Jackson and Hudec 2017). Due to data availability and quality, potassium salts and sulfates (sylvite, carnallite and polyhalite) were grouped (Table 3). Well correlation was completed across the five wells of interest to understand the lateral extent of the facies across the basin where a full petrophysical log suite was unavailable. Thicknesses of individual beds were extracted from the facies log in Petrel and used to calculate the halite purity.

2D seismic reflection data were used to understand the Zechstein salt structures at the well sites. The seismic dataset consisted of legacy data acquired by WesternGeco on behalf of the NSTA in 2015 as part of their Frontiers Programme. Key horizons and

Table 2. *Data availability over the full Zechstein at each well site*

Well	CALI	GR	NPHI	RHOB	DT	Checkshot
26/14-1	✓	✓	✓	✓	✓	
26/12-1	✓	✓	✓	✓	✓	
26/08-1	✓	✓	✓	✓	✓	✓
26/07-1	✓	✓			✓	
26/04-1		✓				

CALI, caliper; GR, gamma ray; NPHI, neutron porosity; RHOB, density; DT, sonic.

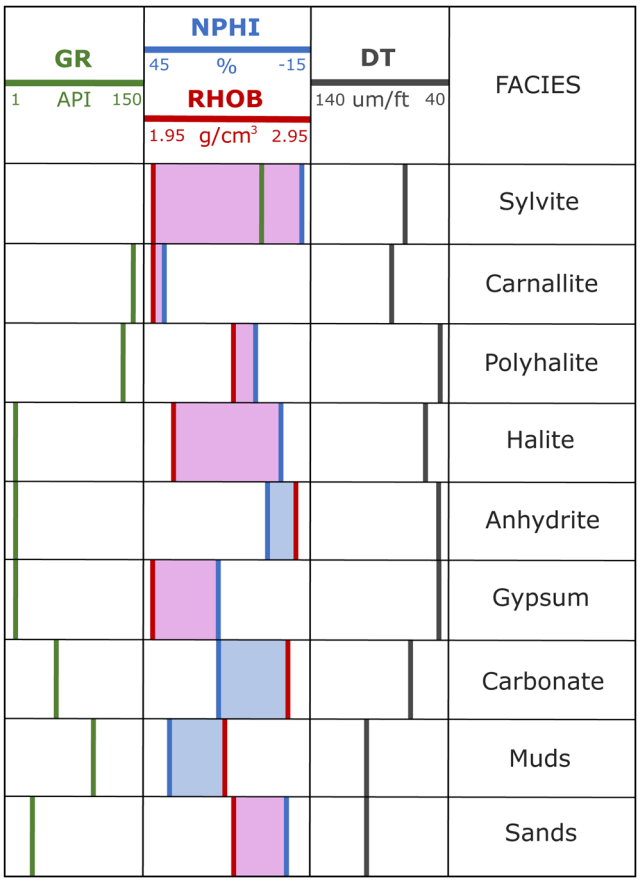

Fig. 3. Petrophysical response of lithologies identified in the Forth Approaches Basin (FAB). CALI, caliper; GR, gamma ray; NPHI, neutron porosity; RHOB, density; DT, sonic.

thickness maps for regional understanding of the FAB were utilized from the NSTA Data Centre (Brackenridge *et al.* 2018). Data were interpreted in Schlumberger's Petrel software, and well checkshot data from 26/08-1 (Table 2) was used to develop a velocity model to convert the seismic data to depth. The seismic data were normal polarity, zero phase.

Results and interpretation

Zechstein well facies

Z5 cycle

The Top Zechstein is typically marked by a log break that indicates a facies change from Triassic mudstone to Permian anhydrite (Figs 4 and 5). The presence of the uppermost Zechstein cycle (Z5) is identified at wells 26/04-1, 07-1 and 08-1 (Fig. 5). However, poor data quality (due to limited log suites and Top Zechstein casing points) leads to some uncertainty in the interpretation of the Top Zechstein at these well sites. The end of well report for 26/04-1 (Glenister *et al.* 2002) places a top Z5 at 398.4 m true vertical depth subsea (TVDSS). However, we shift the top higher to correspond to a probable anhydrite bed at 388 m TVDSS. At 26/07-1 the Top Zechstein is interpreted at 420 m where a decrease in the sonic (DT) log indicates a change to faster velocity facies. The well report for 26/08-1 (Mobil North Sea 1993) places the Top Zechstein at 747 m TVDSS. Here, we tentatively interpret a thin (<1 m) low GR, low neutron porosity (NPHI), high density (RHOB) and low DT layer in the overlying section to represent the anhydritic Z5 Grensanhydrit Formation. Moderate and highly variable GR and DT indicate an interbedded mudstone and anhydrite succession. The Z5 Grenzanhydrit Formation shows a general trend of thinning basinwards from the west and is not present on the eastern margin at wells 26/12-1 and 14-1 (Table 4).

Z4 cycle

The uppermost Z4 cycle, the Aller Halite Formation (AHF), is encountered only at the two wells (26/07-1 and 26/08-1) in the centre of the basin (Table 5). This halite-dominated formation shows a very different petrophysical character to the overlying Grenzanhydrit Formation with a marked decrease in GR and a shift to a more uniform character (Figs 4 and 5). Some higher GR values represent thin heterogeneities. Minor beds of potassium salts, anhydrites and mudstones are interpreted. The upper 52 m of well 26/08-1 is highly heterogeneous. The mud log and geological report (Mobil 1992; Mobil North Sea 1993) describe the upper section as consisting of 'halite with beds of sandstone, siltstone and anhydrite'. A series of sandstone and mudstone beds are interbedded with halite and potassium salts between 760 and 799 m TVDSS. Sand and mud beds are typically less than 2 m thick. Thin (<2 m) anhydrite and anhydritic mud interbeds are more common at the base of the unit. Despite these impurities, halite dominates the AHF with 88% halite purity and a thickness of 221.4 m at well 26/08-1. Clastics are not identified at well 26/07-1; however, thin beds of potassium salts are still present. Here, the AHF is 268 m thick with a halite purity of 87%.

The Z4 Pegmatitanhydrit Formation and the underlying Rozer Salzton unit are manifested by a significant log break and a characteristic petrophysical response (Fig. 4; Table 5). The Pegmatitanhydrit Formation is characterized by a drop in GR, DT and NPHI, and an increase in RHOB. A move to a high GR and high DT (slower) facies represents the Roter Salzton mudstone. At well 26/04-1, the Pegmatitanhydrit and Rozer Salzton formations are interpreted tentatively using the GR. These thin units (generally <15 m combined thickness) are observed at all the well sites, and represent the Top Zechstein at wells 26/12-1 and 26/14-1.

Z3 cycle

The top of the Z3 cycle is marked by a decrease in GR, DT and NPHI, indicating a move to the salts of the Leine Halite Formation (LHF) (Fig. 4; Table 5). The LHF is identified at all five of the wells

Table 3. *Properties of selected evaporites listed in decreasing solubility*

Facies	Chemical formula	Solubility ($g\ l^{-1}$ at 20°C)	GR (° API)	RHOB ($g\ cm^{-3}$)	NPHI (%)	DT (µs/ft)
Sylvite	KCl	340	500	1.86	−3	73
Carnallite	$KClMgCl_2{\cdot}6H_2O$	273	220	1.57	65	79
Polyhalite	$K_2MgCa_2(SO_4)_4{\cdot}2H_2O$		180	2.79	15	57
Halite	NaCl	264	0	2.04	−3	67
Anhydrite	$CaSO_4$	264	0	2.98	−2	48
Gypsum	$CaSO4_2{\cdot}H_2O$	1.97	0	2.35	>60	52

Modified from Jackson and Hudec (2017).

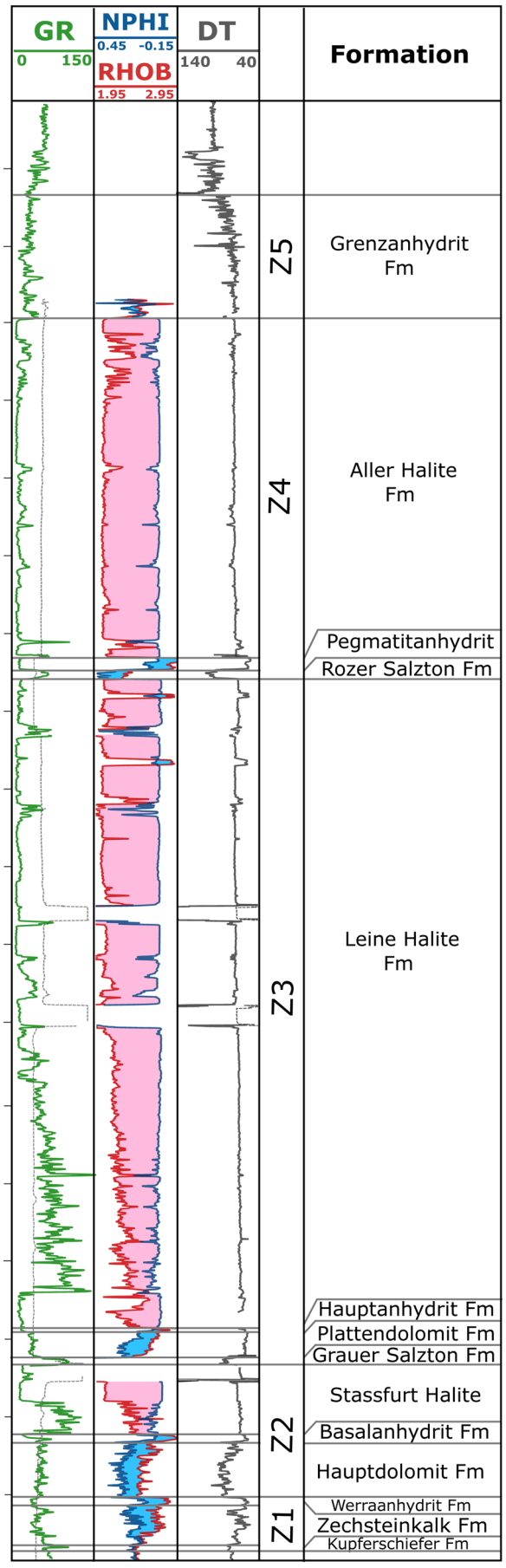

Fig. 4. Frankenstein log of the Zechstein succession in the Forth Approaches Basin (FAB). The logs are taken from wells 26/07-1, 26/08-1 and 26/12-1.

in the FAB and shows considerable variability in log character with depth (Fig. 5). In all wells except 26/04-1, the LHF can be divided into three subunits of different petrophysical character. The upper section, LHF-A, is dominated by halite that is described in the cuttings at well 26/14-1 as hard and crystalline in nature, and white to pinkish and yellowish in colour (Neville and Wreglesworth 1984). Minor impurities are observed on the logs. These are interpreted as thin potassium salt beds with rare anhydrite beds. Potassium salts are typically 1–5 m thick and can be correlated across wells. Anhydrite beds are less common than potassium salts, and are typically less than 2 m thick. Despite these impurities, the majority of the upper LHF consists of halite. Below this upper halite, a change in LHF facies is marked by a strong increase in GR, indicating a dominance of potassium salt beds reaching over 50 m in thickness. This potassium salt-dominated unit is herein named LHF-B. It reaches a maximum thickness of 177 m at the basin margin well 26/14-1 and thins to 55 m to the NW at well 26/07-1. Halite is rare and thin, and potassium salt beds may be separated by thin (<1.5 m) mudstones, particularly towards the base of this unit. The lowermost portion of the LHF consists of a halite-dominated succession. This unit, named LHF-C, is consistent across the four wells sites, ranging from 14 to 26 m thick and with no detectable impurities.

It is not possible to subdivide the LHF into three units at well 26/04-1 (Fig. 5). Individual anhydrite and potassium salts identified elsewhere in the layered sequences in the basin cannot be correlated across to this well. The end of well report (Glenister *et al.* 2002) does not break out the Z3 cycle. We place the top Z3 LHF at 435.6 m TVDSS to correspond to a reduction in GR. A full suite of logs was collected from the lowermost section of the LHF, and its base is clearly seen to correspond to an increase in RHOB and NPHI at 973.6 m TVDSS. This gives a total LHF thickness of 538 m – the thickest of all the wells sites. Poor quality measurement-while-drilling (MWD) GR data do not allow a full interpretation of the LHF at this location. Cuttings suggest that this section is dominated by halite, describing the section as consisting of off-white, white, opaque and translucent brittle halites with rare traces of yellow/brown coloration (Glenister *et al.* 2002). The blocky low GR confirms this interpretation; however, GR increases suggest the presence of minor beds of potassium salt and anhydrite. A tentative halite purity for the entire LHF at well 26/04-1 is calculated at 66%.

At the base of the LHF, the thin (1.4–3.6 m) Hauptanhydrit Formation is identified due to a pronounced increase in RHOB, and this is confirmed by cuttings (Wiggin 1985; Cluff Oil 1986). The underlying Plattendomomit Formation is represented by an increase in NPHI (Fig. 4). The Plattendolomit Formation ranges in thickness from 12.8 to 21.8 m (Table 5) and was a secondary target for several wells. Well 26/04-1 records hydrocarbon saturations of 60–80% through this section (Glenister *et al.* 2002). A GR peak with corresponding increase in DT at the base of the Plattendolomit Formation indicates the thin Grauzer Salzton mudstone that signifies the base of the Z3 cycle (Fig. 4).

Z2–Z1 cycles

The Top Z2 Stassfurt Halite Formation (SHF) is clearly identified as a break in the GR (Fig. 4). The SHF is variable in thickness across the area, ranging between 44.1 and 160.6 m (Table 5). It is also variable in facies across the basin. At well 26/14-1, located on the eastern margin of the FAB, moderate–high GR responses indicate that the SHF is dominated by potassium salts. Two significant halite beds are identified (34 and 14 m thick, respectively). Minor anhydrite is also noted at the base of the formation giving a halite purity of 31%. The other well sites show an upper halite-dominated section and lower potassium salt-dominated section with thin

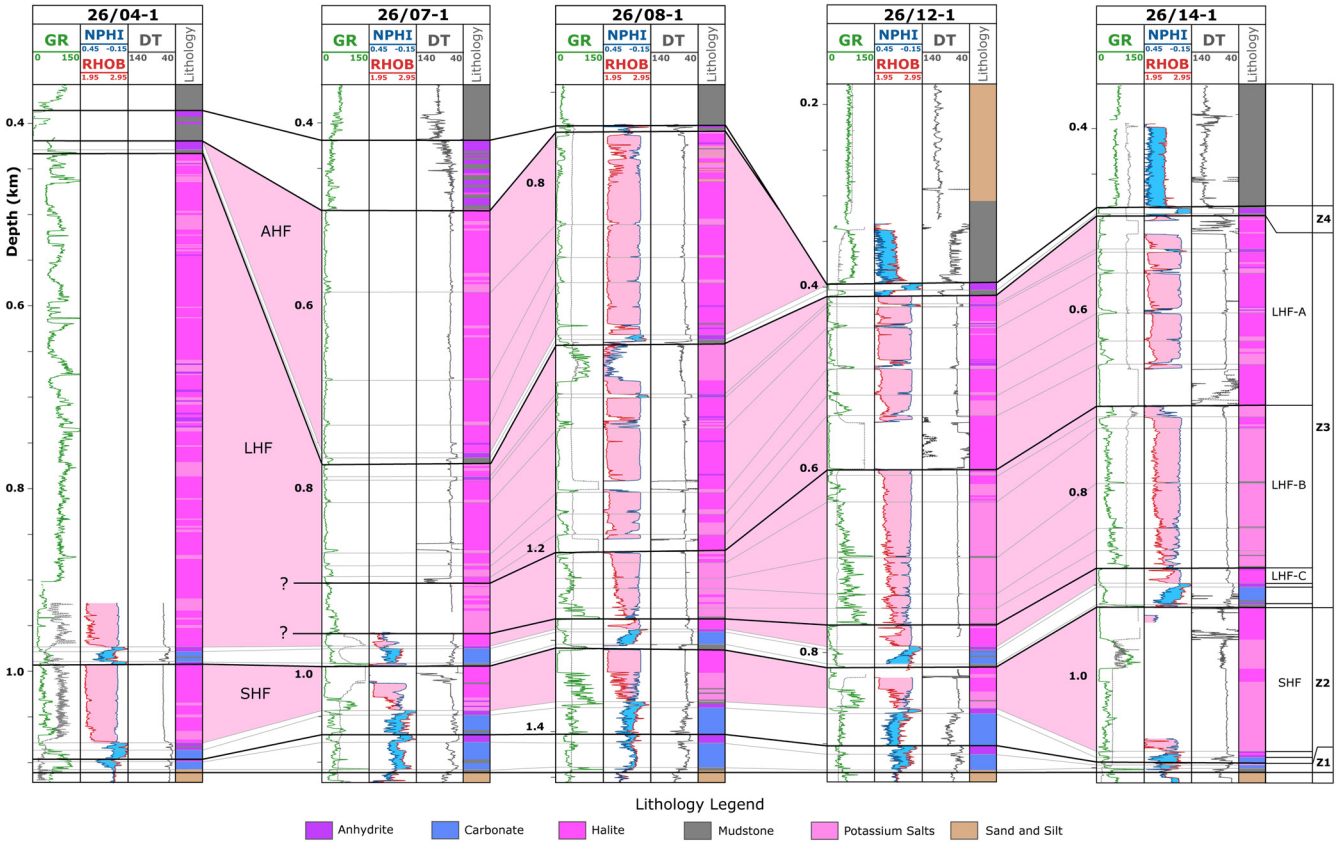

Fig. 5. Well correlation panel. AHF, Aller Halite Formation; LHF, Leine Halite Formation; SHF, Stassfurt Halite Formation.

mudstones and rare anhydrite (Fig. 5). Halite purity generally increases from SE to NW, to a maximum of 82.8% at well 26/04-1.

The underlying Basal Anhydrite Formation and Hauptdolomit Formation complete the Z2 cycle. There is uncertainty in distinguishing the Z2 and Z1 cycles at some well sites; however, Z2 Basal Anhydrite and Hauptdolomit formations, and the Z1 Werraanhydrit and Zechsteinkalk formations are broadly represented by a pronounced increase in NPHI and RHOB. Anhydrites are distinguished based on their lower GR and DT (faster) values (Fig. 4). The dolomites of the Hauptdolomit and Zechsteinkalk formations are thickest in the basin centre at wells 26/07-1, 08-1 and 12-1 (Fig. 5), reaching a maximum thickness of 37.1. An oil show was recorded in the Hauptdolomit Formation at well 26/07-1 (Wiggin 1985).

A GR peak commonly seen underlying the Zechsteinkalk Formation represents the thin Kupferschiefer Formation at the base of the Zechstein. The Kupferschiefer Formation is absent at well 26/04-1, with the end of well report suggesting that it is absent due to downslope remobilization (Glenister *et al.* 2002). The Base Zechstein is deepest in the centre of the basin at well 26/08-1 where it reaches 1441.4 m TVDSS (Table 5).

Zechstein seismic facies and structure

Well 26/14-1 is located on the eastern margin of the FAB (Fig. 1). At this site the Top Zechstein is 417.9 m below the seabed and reaches a total thickness of 615.7 m (Table 4). The seismic data show evidence for minor halokinesis close to the well (Fig. 6) but in general the Zechstein exhibits moderate amplitude reflections that can be traced laterally, indicating a layered or bedded succession. The Zechstein sits atop the Permian Rotliegend, which unconformably overlies highly fractured Devonian clastics (Neville and Wreglesworth 1984). This suggests that the Permian sits on a palaeohigh at this site (Cartwright *et al.* 2001). Well 26/12-1 is located 21.5 km west of 26/14-1 and sits along strike on the same palaeohigh (Fig. 1). The Top Zechstein sits 350.9 m below the seabed. This well site shows the thinnest Zechstein succession at just 532.7 m thick (Table 4). The Permian Rotliegend is also absent at this well and the Zechstein unconformably overlies highly altered Devonian sandstones (Fig. 7) (Cluff Oil 1986). The seismic facies show moderate-amplitude reflections that can be traced laterally, indicating a layered evaporite succession (Fig. 6).

Table 4. *Thickness at each well site*

	04-1	07-1	08-1	12-1	14-1
Sea level	67.7	64.9	56.7	44.5	68.6
Post-Zechstein overburden	351.6	355.1	681.3	350.9	417.9
Z5	31.3	74.1	6.4	0	0
Z4	16.4	276.8	231.3	13.7	7.9
Z3	557.1	224.2	335.6	407.8	429.5
Z2	102.9	75.4	94.3	85.4	170.8
Z1	12.0	37.5	36.2	25.8	7.5
Sum of Zechstein	719.7	688.0	703.8	532.7	615.7

Table 5. *Zechstein well tops and formation thickness as determined in this study, and the petrophysical character of each formation*

	Formation		Well 26/04-1	26/07-1	26/08-1	26/12-1	26/14-1	Petrophysical response and facies interpretation
Z5	Grenzanhydrit Formation	Top depth (m TVDSS)	387.9	420.0	737.6	Absent	Absent	Low–moderate GR, low NPHI, high RHOB and low DT layers within a variable succession representing interbedded anhydrite and mudstones
		Thickness (m)	31.4	74.1	6.4			
Z4	Aller Halite Formation	Top depth (m TVDSS)	Absent	494.1	744.0	Absent	Absent	Low blocky GR, and low RHOB, NPHI and DT sections are interpreted as halite. Sections with low GR and NPHI, moderate RHOB, and very low DT are interpreted as anhydrite. Potassium salts are identified based on an increase in GR and decrease in RHOB. Sections with low–moderate GR, RHOB and NPHI are classified as sands and siltstones
		Thickness (m)		268.4	221.5			
	Pegmatitanhydrit Formation	Top depth (m TVDSS)	419.3	762.5	965.5	395.4	486.5	Characterized by a drop in DT and NPHI, and an increase in RHOB representing anhydrite
		Thickness (m)	12.3	5.0	7.0	7.8	6.4	
	Roter Salzton Formation	Top depth (m TVDSS)	432.6	767.5	972.5	403.2	492.9	High GR, and low-velocity (high DT) mudstone and anhydritic mudstones. Where data are available, high NPHI and moderate RHOB observed
		Thickness (m)	4.1	3.4	2.8	5.9	1.5	
Z3	Leine Halite Formation	Top depth (m TVDSS)	435.6	770.9	975.3	409.2	494.4	Low GR, and low RHOB, NPHI and DT sections are interpreted as halite. Sections with low GR and NPHI, moderate RHOB, and very low DT are interpreted as anhydrite. Potassium salts are identified based on an increase in GR and a decrease in RHOB
		Thickness (m)	538.0	201.7	312.4	384.0	402.9	
	Hauptanhydrit Formation	Top depth (m TVDSS)	973.6	972.6	1287.7	793.1	897.3	Characterized by a drop in DT and NPHI, and an increase in RHOB representing anhydrite
		Thickness (m)	2.8	1.5	1.4	3.6	2.8	
	Plattendolomit Formation	Top depth (m TVDSS)	976.5	974.1	1289.1	796.7	900.1	An increase in GR and NPHI, and a decrease in RHOB marking a facies change to dolomite
		Thickness (m)	12.8	18.3	17.0	18.7	21.8	
	Grauer Salzton Formation	Top depth (m TVDSS)	989.3	992.4	1306.1	815.4	921.9	GR peak with corresponding high DT representing mudstones
		Thickness (m)	3.4	2.7	4.8	1.5	2.0	
Z2	Stassfurt Halite Formation	Top depth (m TVDSS)	992.7	995.1	1310.9	816.9	923.9	Low GR, and low RHOB, NPHI and DT sections interpreted as halite. Potassium salts are identified based on an increase in GR and a decrease in RHOB
		Thickness (m)	84.8	47.4	55.9	44.1	160.6	
	Basalanhydrit Formation	Top depth (m TVDSS)	1077.6	1042.4	1366.8	861.0	1084.5	Characterized by a drop in DT and an increase in RHOB representing anhydrite
		Thickness (m)	8.2	4.5	5.8	4.3	2.2	
	Hauptdolomit Formation	Top depth (m TVDSS)	1085.7	1047.0	1372.6	865.3	1086.7	An increase in GR, NPHI and DT, and a decrease in RHOB marking a facies change to dolomite
		Thickness (m)	9.9	23.5	32.6	37.1	8.0	
Z1	Werraanhyrtit Formation	Top depth (m TVDSS)	1095.6	1070.5	1405.2	902.3	1094.7	A drop in DT and NPHI, and an increase in RHOB representing anhydrite
		Thickness (m)	1.0	5.0	5.5	7.6	7.5	
	Zechsteinkalk Formation	Top depth (m TVDSS)	1096.6	1075.5	1410.7	909.9	1096.1	An increase in NPHI and DT, and a decrease in RHOB marking a facies change to dolomite
		Thickness (m)	11.0	31.5	29.9	17.3	1.4	
	Kupferschiefer Formation	Top depth (m TVDSS)	Absent	1107.0	1440.6	927.3	1100.8	Strong GR peak with a corresponding high DT representing mudstones
		Thickness (m)		1.0	0.8	0.9	4.7	
Base Zechstein			1107.6	1108.0	1441.4	928.1	1102.2	

Well 26/08-1 is located in the centre of the FAB (Fig. 1). As a result, the Zechstein is buried deepest at this location at 681 m TVDSS. This well also penetrates the thickest succession of Zechstein (703 m) (Table 4). Rotliegend sandstone, 390 m thick, underlies the Zechstein with a thick Upper and Lower Carboniferous package encountered before terminating at 3435 m TVDSS (Fig. 7) (Mobil North Sea 1993). The well penetrated the Zechstein between two salt diapir structures in a section of uniform thickness (Fig. 6). The Zechstein shows variable seismic facies. The upper portion is very low amplitude to transparent in nature. This seismic unit pinches out away from the well location and is not observed at the previously described well sites. A high-amplitude soft acoustic impedance event separates the transparent seismic facies from the lower Zechstein facies, showing moderate-amplitude, semi-continuous reflections (Fig. 6) that indicate a layered sequence.

Well 26/07-1 is located just 1 km west of 26/08-1 (Fig. 1). The Zechstein is not as deeply buried as in the nearby 26/08-1, at just 355 m. The Zechstein Group reaches a thickness of 668 m (Table 4). The well encountered Permian Rotliegend sandstones below the Zechstein (Fig. 7). The Upper Carboniferous was absent, and the well TD-ed in Lower Carboniferous interbedded sands, shales and coals. This indicates that the well sits within the basin centre but is closer to the western margin of the FAB than well 26/08-1. The seismic data reveal that the well was drilled adjacent to a salt diapir (Fig. 6). As with well 26/08-1, the Zechstein seismic facies can be divided into an upper unit of low-amplitude to transparent discontinuous reflections and a lower unit with moderate-amplitude, semi-continuous reflections. These units are separated by a high-amplitude, soft acoustic impedance contrast. Seismic mapping shows that the upper unit

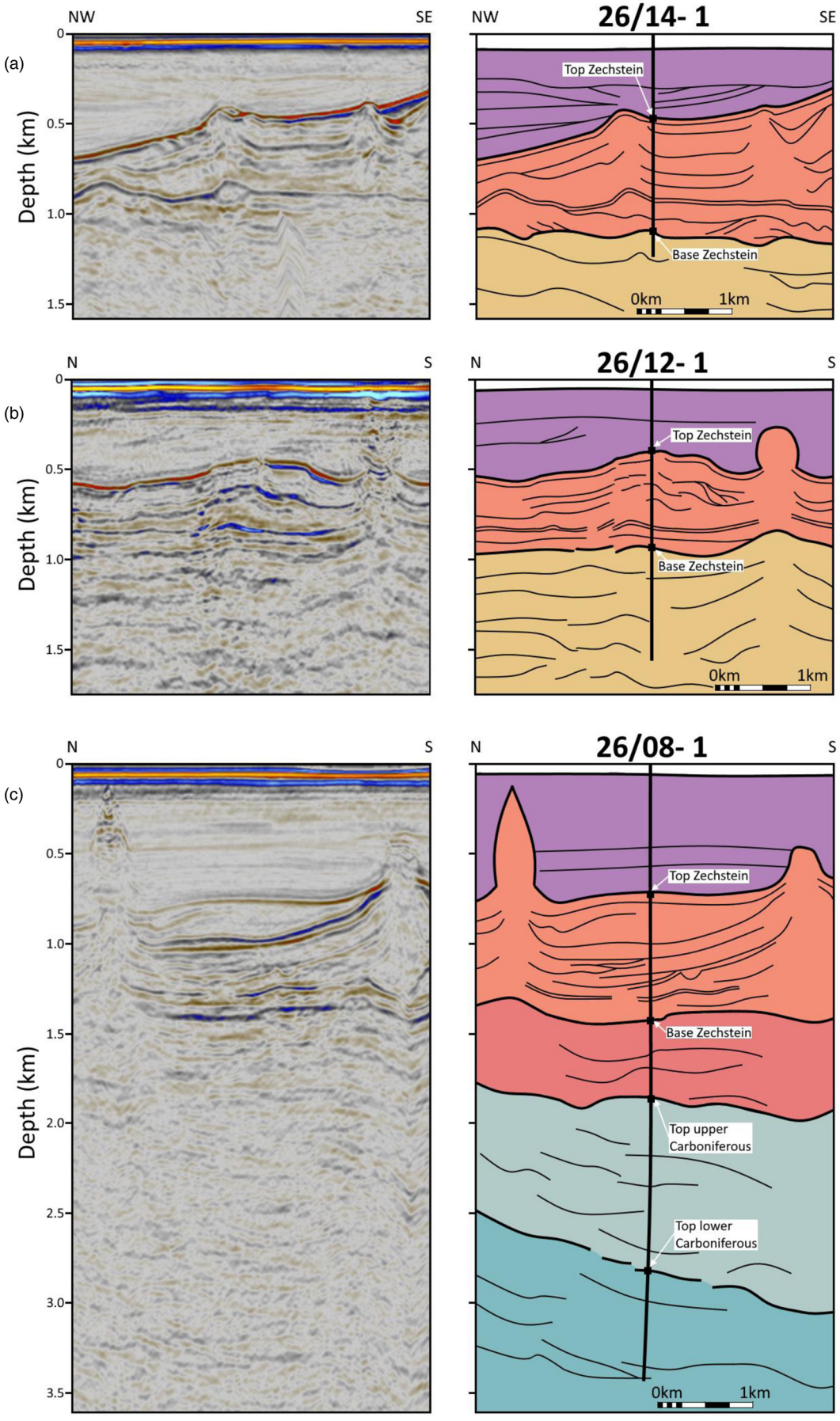

Fig. 6. Seismic section across each well location uninterpreted (left) and interpreted (right) with well tops. Seismic in depth.

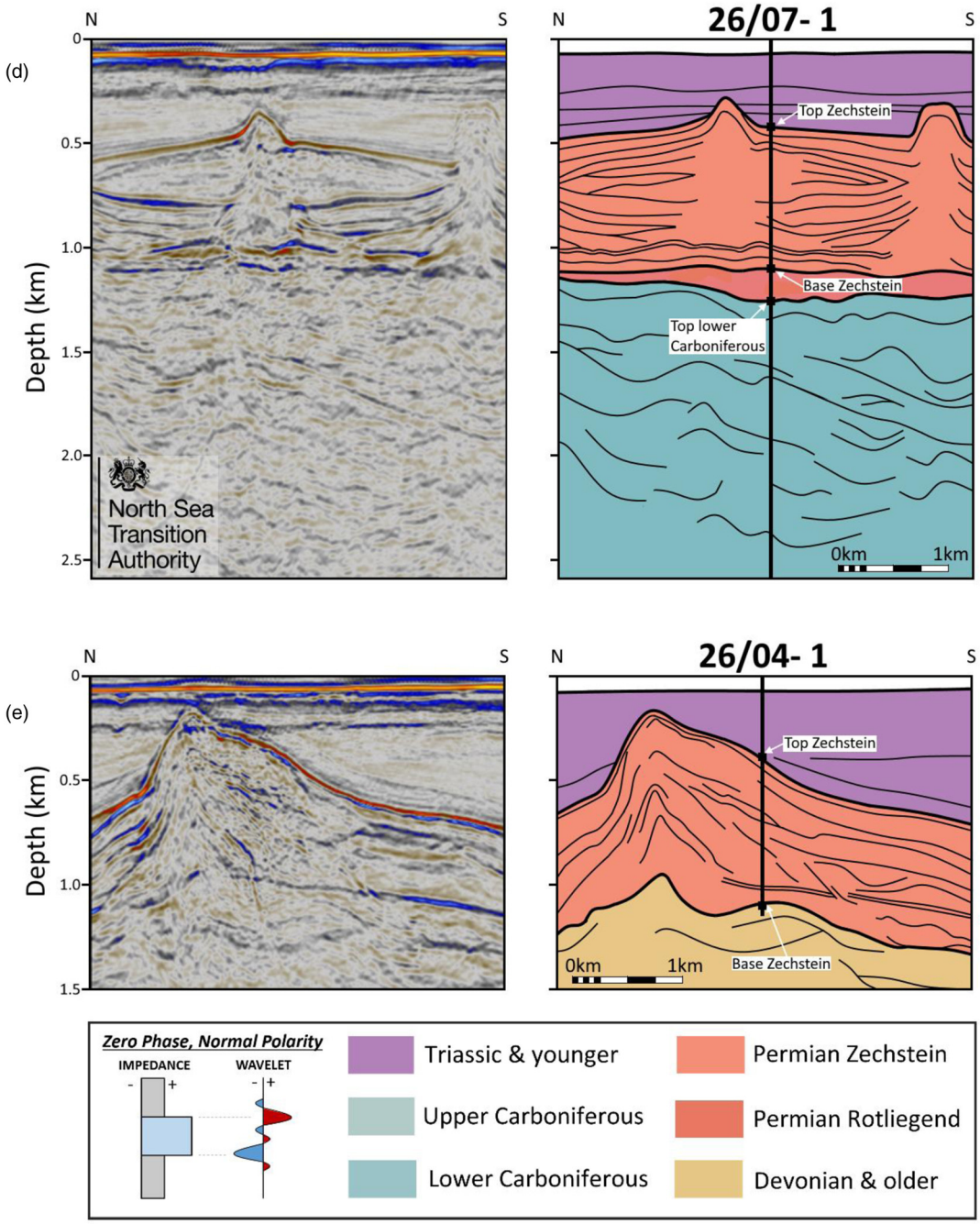

Fig. 6. Continued.

thins and pinches out away from the well and is interpreted to represent the AHF.

The final well drilled in the FAB targeted a Base Zechstein high in the north of the basin (Fig. 1). The Top Zechstein was encountered at 351.6 m below the seabed and the primary target, the Z2 Hauptdolomit Formation, is seen at 1085.7 m TVDSS. The secondary target, the Permian Rotliegend, was absent, and the well TD-ed within metamorphosed Devonian sandstones (Fig. 7). The absence of Rotliegend and Carboniferous stratigraphy here indicates that a palaeohigh was present at the site at the time of Zechstein deposition. The Zechstein is at a similar depth and of a similar thickness to that observed at well 26/07-1; however, the seismic data show a very different response. The well drilled the southern flank of a salt diapir (Fig. 6). The seismic facies are discontinuous to chaotic, indicating strong deformation due to halokinesis and the resultant disappearance of horizontal–subhorizontal bedding.

Variability of halite facies in the FAB

Zechstein facies in the FAB

Zechstein thickness is variable over the basin, and this is evidenced in both the well and seismic data, varying between 523.7 and 703.4 m at the well sites (Table 4; Fig. 4). The seismic data reveal that variations in Zechstein thickness are driven by a mix of depositional thickness differences and subsequent halokinesis (Fig. 6). Four of the wells penetrate the Zechstein at sites where the seismic facies are layered. Previous studies indicate that salt diapirs are common within the FAB (Cartwright *et al.* 2001; Brackenridge *et al.* 2020); however, no wells have penetrated the full thickness of a diapir. Well 26/04-1 penetrates the flank of a salt diapir structure (Fig. 6) and provides important information about the facies within these salt structures.

The distribution and thickness of the Z1–Z5 cycles vary over the FAB (Fig. 7). Z1 is encountered in all five wells, with a thin (<15 m)

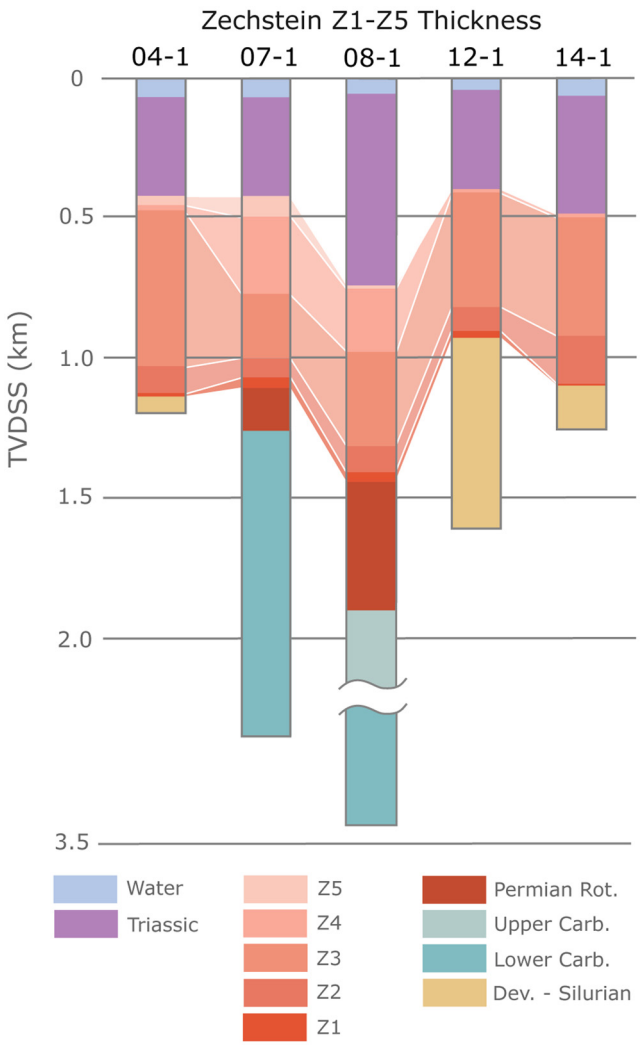

Fig. 7. Zechstein thickness and Z1–Z5 variability across the studied wells.

Z1 seen on the basin margin thickening to 38 m in the basin centre (Table 4; Fig. 7). The opposite trend is observed for the Z2 cycle, which is thickest at the wells located on the basin margins (171 m at well 26/14-1) (Fig. 7). The Z3 cycle is dominated by the LHF (Table 4). As a result, the Z3 cycle is strongly influenced by halokinesis and reaches over 550 m at well 26/04-1 located on the flank of a salt diapir (Table 4). The Z3 cycle dominates the Zechstein section at most well sites (Fig. 7). The Z4 sequence is seen at all wells but is highly variable in thickness. Where the AHF is present at wells 26/07-1 and 26/08-1, the Z4 cycle reaches 231 and 276 m, respectively. Z5 is not observed at wells 26/12-1 and 26/14-1, and reaches a maximum thickness of 74 m at well 26/07-1 on the western margin of the basin (Fig. 7).

The pre-Zechstein basin topography therefore appears to have a complex control on the distribution of the Zechstein cycles. The basin-bounding fault to the SE of the FAB exerts a strong control on dolomite growth in the Z1 and Z2 cycles at well 26/14-1. In the hanging wall, Z4 and Z5 cycles appear to build out from the west, and the Z5 cycle is not seen at wells in the east of the study.

Halite depth and formation thicknesses

Within the Zechstein, three significant halite sequences are identified: (1) the Z2 Stassfurt Halite Formation (SHF); (2) the Z3 Leine Halite Formation (LHF); and (3) the Z4 Aller Halite Formation (AHF) (Figs 4 and 5). The SHF shows variable thickness across the basin, ranging from 44 to 161 m (Fig. 8). It is thickest on the basin margins (Table 6). The SHF is the thinnest and most deeply buried of the three halite formations identified in the FAB, reaching up to 1311 m TVDSS (Table 6). The LHF is thickest at well 26/04-1 where a salt diapir has formed. It reaches 558 m thick on the flank of this salt diapir (Table 6); however, the seismic data indicate that the halite increases in thickness to the north where the diapir reaches maximum thickness (Fig. 6). Within layered sequences, the LHF thickens towards the southern margin of the FAB where it reaches 403 m at well 26/14-1 (Fig. 8; Table 6). The depth of burial at the well sites ranges from 409 to 744 m for the LHF. The youngest halite formation, AHF, is only observed at wells 26/07-1 and 26/08-1, located in the centre of the basin, where it reaches 268 and 222 m, respectively (Fig. 8). Well 26/08-1 in the centre of the basin is most deeply buried at 744 m TVDSS (Table 6).

Halite heterogeneity

Detailed petrophysical analysis of the SHF, LHF and AHF reveals that there are heterogeneities in lithology. Lithologies have been interpreted based on their GR, NPHI, RHOB and DT responses (Figs 3 and 4). All halite formations consist of halite with potassium salts, and minor anhydrites, mudstones and sandstones.

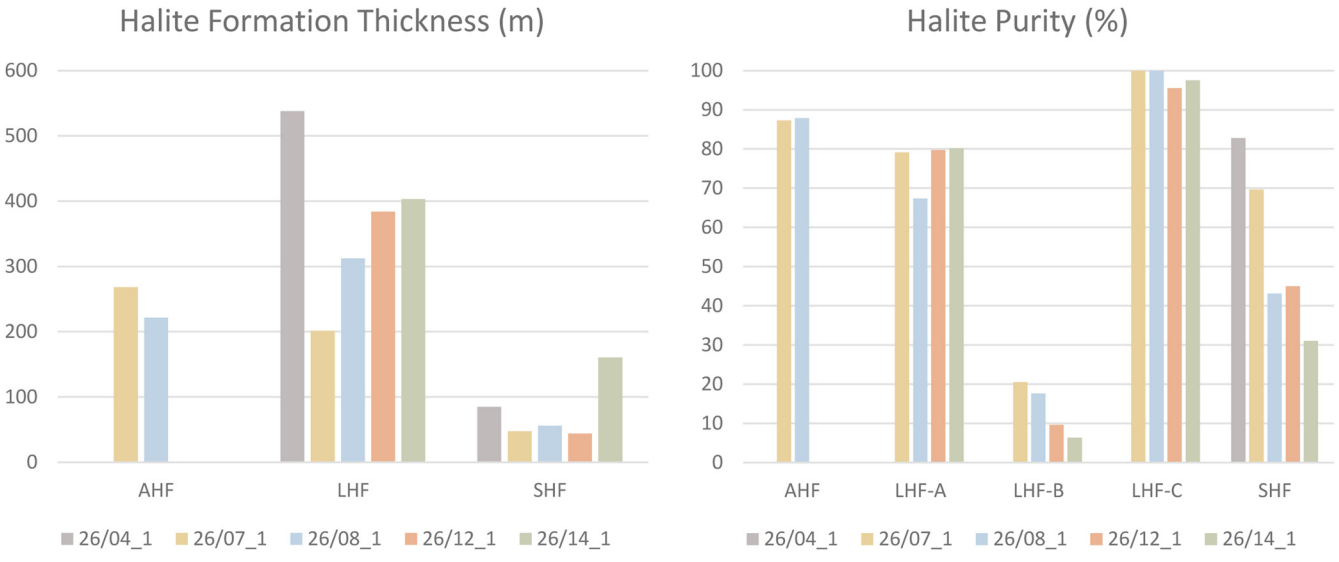

Fig. 8. Aller Halite Formation (AHF), Leine Halite Formation (LHF) and Stassfurt Halite Formation (SHF) thickness and halite purity at each well site.

Table 6. *Depth and thickness for the key halite formations in the Forth Approaches Basin (FAB)*

		Well				
		26/04-1	26/07-1	26/08-1	26/12-1	26/14-1
AHF	Top depth (m TVDSS)	?	494	744	Absent	Absent
	Thickness (m)		268	222		
LHF total	Top depth (m TVDSS)	436	771	975	409	494
	Thickness (m)	538	202	312	384	403
LHF-A	Top depth (m TVDSS)	?	771	975	409	494
	Thickness (m)		132	226	189	209
LHF-B	Top depth (m TVDSS)	?	903	1201	598	704
	Thickness (m)		55	75	172	178
LHF-C	Top depth (m TVDSS)	?	958	1276	771	881
	Thickness (m)		15	12	23	16
SHF total	Top depth (m TVDSS)	993	995	1311	817	924
	Thickness (m)	85	47	56	44	161

Depth and thickness are rounded to the nearest metre. AHF, Aller Halite Formation; LHF, Leine Halite Formation; SHF, Stassfurt Halite Formation.

The SHF shows the most variable halite purity values. Halite purity is highest in the salt diapir at well 26/04-1 (85%) and lowest at site 26/14-1 in the southeast (31%) (Fig. 8). Based on changes in the thickness and nature of heterogeneities, the LHF can be divided into three distinct subunits: LHF-A–LHF-C (Figs 5 and 9). LHF-A represents the upper halite-dominated unit. Unlike the overlying AHF, there is a notable absence of clastic beds in this unit (Fig. 9). LHF-A is thickest in the centre of the basin at well 26/08-1 where it reaches 226 m. It is distinguished from underlying LHF-B due to its halite purity, which shows a consistent purity of 80% across all well sites except 26/08-1 (67%) (Fig. 8). This contrasts with LHF-B, which is dominated by potassium salts (Figs 5 and 9). LHF-B thickens to the south from 55 m at well 26/07-1 to 177.6 m at 26/14-1 (Fig. 9). All wells show a thin (<25 m) halite layer at the base of the LHF: LHF-C (Fig. 9). The three subunits within the LHF cannot be correlated to well 26/04-1 (Fig. 5) and we conclude that the LHF has been significantly deformed at this well locality due to halokinesis. The SHF is the only other halite that reaches significant thickness in the FAB. Heterogeneities are highly variable over the FAB (Fig. 8). Well 26/04-1, located on the salt diapir flank, has the highest halite purity at 84.8%. Most wells show purities less than 50%, with potassium salts dominating at many wells. Minor mudstones and anhydrites are most common in the basin centre.

The data quality is insufficient to distinguish the type of potassium salts in detail; however, the petrophysical response (Fig. 3) and end of well reports indicate that interbeds of carnalite, polyhalite and sylvite are all present in the FAB. Interbeds of these potassium salts occurs on multiple scales (reaching >50 m thick within LHF-B). These chemical heterogeneities represent changes in the seawater chemistry at the time of deposition, and indicate that flooding and evaporation cycles occurred on a smaller scale than in

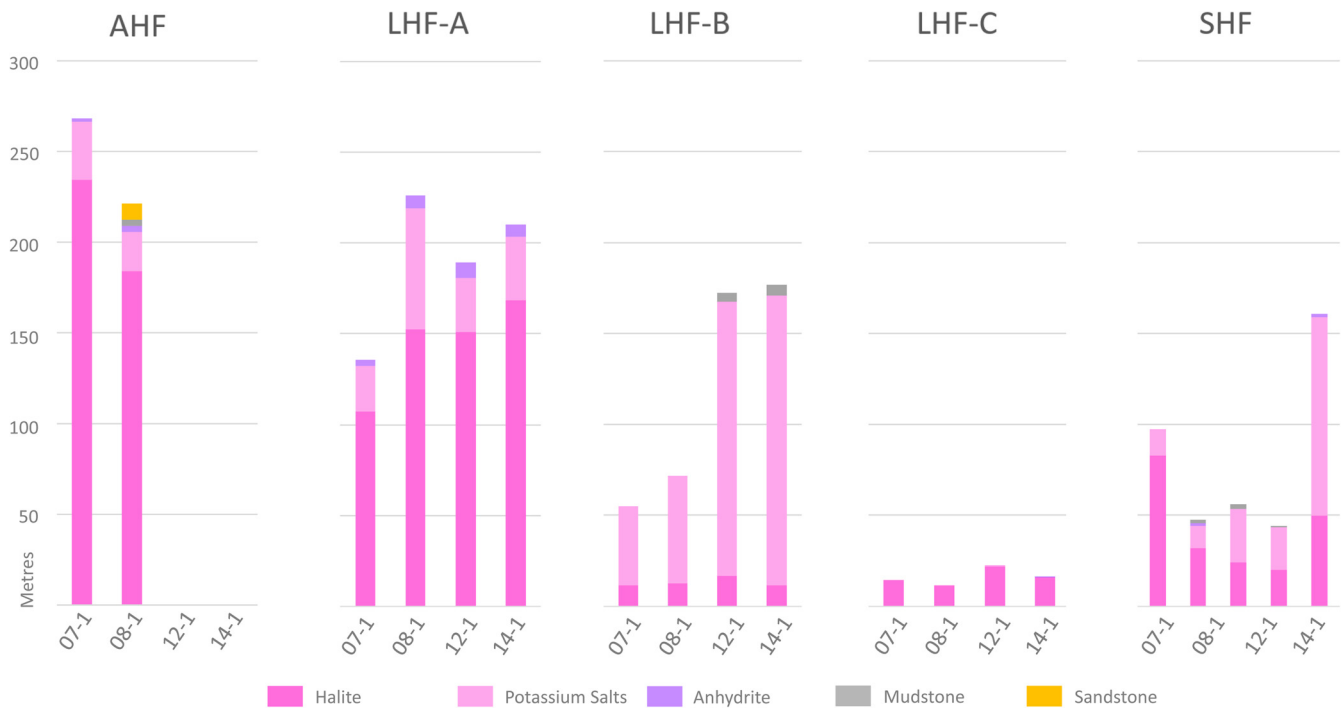

Fig. 9. Aller Halite Formation (AHF), Leine Halite Formation (LHF) and Stassfurt Halite Formation (SHF) thickness and halite purity at each well site showing the lithological breakdown. Thicknesses are in metres. 07-1, well 26/07-1; 08-1, well 26/08-1; 12-1, well 26/12-1; 14-1, well 26/14-1.

the five major Z cycles. In addition to the clear chemical heterogeneity observed across the halite formations, lithological heterogeneities are observed at key intervals. Most notably, the AHF is characterized by clastic sediments interbedded with halite.

The AHF is observed at only two well sites but shows similar halite purity values (Fig. 8). This suggests that Z4 halite precipitation was restricted to local basins but well locations 26/07-1 and 26/08-1 were in communication at the time of precipitation. Despite heterogeneities in the LHF, units can be correlated across the FAB wells (with the exception of 26/04-1 where later halokinesis has deformed the unit). The thickness of the LHF-A–LHF-C units is variable; however, the halite purity of each unit remains consistent across the basin (Fig. 8). This indicates that the LHF was deposited in a broad basin. This contrasts with the SHF that shows notable differences in halite purity across the well sites (Fig. 8), suggesting that the FAB consisted of a series of separate mini-basins experiencing different flooding events at this time. Later halokinesis has locally deformed bedding within the Zechstein halite formations (e.g. 26/04-1), making halite heterogeneity studies challenging, and reducing the ability to predict likely chemical and lithological impurities.

Discussion

Suitability of the FAB halites for hydrogen storage

This research aimed to assess the geological adequacy of the Zechstein salt for hydrogen storage in the Forth Approaches Basin (FAB). For a site to be suitable for salt cavern storage, the targeted halite store must fulfil several geological criteria (Smith *et al.* 2005). Key controls to assess potential storage sites are: (a) halite thickness – beds should be sufficiently thick to allow an economic cavern volume with adequate roof and floor thickness to ensure structural integrity (Williams *et al.* 2022); (b) burial depth – the halite should be sufficiently buried to avoid gas outbursts but not so deep as to allow pressure-induced salt creep, which will compromise cavern integrity (Smith *et al.* 2005; Tarkowski 2019); and (c) halite purity – intra-salt heterogeneities can impact well and cavern integrity, can react with injected fluids, and can control the geometry of the salt cavern, thus affecting capacity and cavern stability (Warren 2017; Duffy *et al.* 2022).

Halite thickness

The European natural gas cavern industry has set out standard engineering practice for future salt caverns and stated that cavern volumes should be in excess of 500 000 m^3 (Crotogino 2022). The cavern height/diameter ratio should be >0.5 (Allsop *et al.* 2023). The cavern should also be located away from the edge of the salt body to ensure seal integrity (Wang *et al.* 2015). The roof of the cavern should be a minimum of 75% of the cavern diameter away from the top of the salt body, and 20% of the cavern diameter from the base (Wang *et al.* 2015; Caglayan *et al.* 2020). With this in mind, the minimum thickness for the safe and economic storage of hydrogen with salt bodies is calculated as 205 m, with a cavern height of 140 m and a diameter of 67.46 m. Smith *et al.* (2005) estimated that a halite thickness greater than 300 m is recommended for the cavern to be of economical capacity for gas storage, and this is used herein to ensure operational safety and to account for the added costs of an offshore installation. Existing storage sites within layered evaporites are typically smaller: the onshore salt caverns at Teeside are located within a 50 m-thick halite layer (Crotogino 2022). Caverns within salt diapirs can exceed 300 m and reach heights of up to 500 m (Michalski *et al.* 2017).

Based on the well data in the FAB, the only halite formation to reach sufficient thickness for effective and economic hydrogen storage is the Leine Halite Formation (LHF) (Table 6; Fig. 8). The LHF has a thickness greater than 300 m at all the well sites examined, except for well 26/07-1 (Table 6; Fig. 8). However, where the LHF is layered it can be subdivided into three distinct units (LHF-A–LHF-C). LHF-B is dominated by potassium salts and is unsuitable for salt solution mining. LHF-C is less than 25 m thick, and therefore is also unsuitable for further investigation. LHF-A is halite dominated, reaching a maximum of 226 m thick at well 26/08-1 (Table 6; Fig. 9). The overlying Aller Halite Formation (AHF) is only identified at wells 26/07-1 and 26/08-1 (Figs 5 and 9), where it reaches thicknesses of 273 and 231 m, respectively. The AHF and LHF are separated by the thin (<10 m) Pegmatitanhydrit and Roter Salzton formations. The underlying LHF-A has thicknesses of 132 and 226 m at wells 26/07-1 and 26/08-1, respectively, therefore suggesting that the combined AHF and LHF-A halites are sufficiently thick at these two well sites for further investigation for solution mining. AHF is absent from wells 26/12-1 and 14-1, where the LHF-A is *c.* 200 m thick. Therefore, these well sites are not suitable for solution mining for subsurface storage.

The LHF at well 26/04-1 cannot be divided into subunits, and is dominated by halite throughout. This is thought to be due to its location on the flank of a salt diapir. The LHF reaches a total thickness of 558 m (Table 6; Fig. 8), making it an excellent candidate for salt solution mining. The seismic interpretation (Fig. 5) shows that none of the wells penetrate the thickest sections of the Zechstein but were drilled adjacent or on the flanks of diapirs. However, halokinesis is common across the FAB (Fig. 6) (Cartwright *et al.* 2001). It can therefore be expected that away from the wells, the LHF has further potential to exceed the sufficient thickness required for economic storage capacity within salt structures. The Stassfurt Halite Formation (SHF) reaches a maximum thickness of 161 m but is generally less than 100 m at the well sites examined in this study (Table 6; Fig. 8). It is therefore unsuitable for further investigation as a potential formation for hydrogen storage.

Halite depth

A site's suitability for solution mining is also determined by the depth to the top and base halite. The depth to halite must be sufficiently deep to avoid gas outbursts (Smith *et al.* 2005). Burial must also be shallow enough to avoid salt creep: beyond 2000 m increased pressure and temperature result in highly mobile salt, and cavern deformation is unmanageable (Muhammed *et al.* 2022). The depth also exerts a control on the economic feasibility of a cavern site, with more cushion gas required in a deeper cavern to account for increased pressures (Zivar *et al.* 2021). Previous studies suggest a minimum burial depth to top halite as 300 m (Smith *et al.* 2005) and a maximum burial as 1500 m (Tarkowski 2019).

Based on the well data from the FAB, the AHF, LHF and SHF are within the required depth ranges for solution mining (Table 6; Fig. 10). The seismic data show variability in the depth of Zechstein burial across the FAB. The Zechstein is most deeply buried at well 26/08-1, located in the centre of the basin. Here the top AHF is 744 m TVDSS (Table 6). Wells located around the margins of the basin have top halite depths of 400–500 m. Top halite is shallowest at well 26/04-1, located on the flank of a salt diapir at 436 m TVDSS. Although the salt diapir is an attractive target for salt solution mining due to its halite thickness and purity, the seismic interpretation shows that the crest of the diapir is close to the seabed (Fig. 6). Care must be taken to accurately map the depth of top halite when assessing the suitability of salt structures for solution mining; however, much of the FAB halites sit within the optimal operational window (Fig. 10). This arguably makes the FAB unique in the Central North Sea, where much of the Zechstein has been more deeply buried due to Late Jurassic extension and is therefore unsuitable for salt cavern placement.

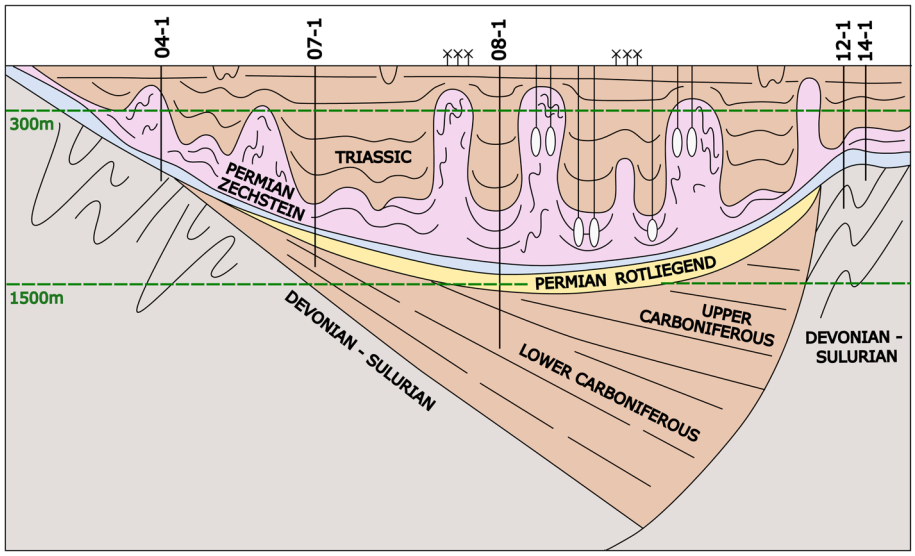

Fig. 10. Simplified schematic cross-section through the Forth Approaches Basin (FAB) indicating locations suitable for salt dissolution mining for hydrogen storage close to surface infrastructure. A suitable depth range for salt cavern mining indicated is in green. Adapted from Cartwright *et al.* (2001). Not to scale. 04-1, well 26/04-1 07-1, well 26/07-1; 08-1, well 26/08-1; 12-1, well 26/12-1; 14-1, well 26/14-1.

Halite purity

Salt formations are known to be highly homogeneous bodies consisting of multiple evaporites (potassium salts and sulfates such as carnallite, sylvite or polyhalite). These are called 'geochemical' heterogeneities. Salts can also be interbedded with other 'lithological' heterogeneities (insoluble material such as anhydrite, clastics or carbonates) (Jackson and Hudec 2017; Rowan *et al.* 2019). These heterogeneities can impact well and cavern integrity (Warren 2017; Duffy *et al.* 2022). Potassium salts (such as carnallite) are problematic for salt solution mining due to their highly soluble nature (Tarkowski 2019). There is potential for carnallite units to dissolve quicker than the surrounding halite, creating uneven cavern shapes and points of weakness. Any non-salt beds are more likely to collapse and collect at the base of the cavern, and the presence of different minerals may make the salt more likely to fracture (Clave *et al.* 2019). Insoluble layers such as anhydrite, clastics or carbonates tend to form ledges that later collapse and can damage equipment (Warren 2016). The relative higher density of anhydrite results in beds dissolving slower than the halite and consequently creating irregular cavern shapes. Sand and mudstone layers will not dissolve and remain as ledges in the salt wall prone to collapse. Furthermore, insoluble material may act as migration routes and form leak points for stored fluids (Warren 2017).

Variations in halite purity are observed across the wells in this study. The SHF shows the largest ranges in halite purity across the basin, varying from 31 to 83% (Fig. 8), with potassium salts the main secondary facies. This indicates that the SHF was probably precipitated within isolated mini-basins with different hydrological histories. The log response indicates polyhalite as the main impurity within the SHF (Fig. 3). Due to the limited thickness of the unit, it is not investigated further.

Carnalite and polyhalite are the primary heterogeneities identified in the LHF. Where the sequence is layered, upper and lower halite-dominated units LHF-A and LHF-C are separated by a potassium salt-dominated unit that can be correlated regionally across the wells (Fig. 5). This geochemical heterogeneity is recorded in geological completion reports but this petrophysical study concludes that their extent and significance is larger than that of the original interpretation. Minor anhydrite and mudstone beds are also identified within the LHF (Fig. 9) but they are typically less than 4 m in thickness and therefore present a minimal risk to potential salt caverns in the FAB.

The LHF at well 26/04-1, located on the flank of a salt diapir, is significantly different in character to the other well sites (Figs 6 and 10). Impurities are observed; however, potassium salts appear thinner and equally dispersed within the halite. Predictability of heterogeneities within salt structures remains a challenge for cavern placement. Duffy *et al.* (2022) suggested that a good understanding of the undeformed evaporite sequence adjacent to salt structures could aid de-risking the internal deformation within salt diapirs for solution mining. The limited log suite at well 26/04-1 results in remaining uncertainly as to the nature of the halites within salt structures of the FAB.

The AHF has some of the highest halite purities identified in this study (Fig. 8) with only minor polyhalite beds identified. Thin interbeds of sandstone and mudstone are common in the uppermost AHF at well 26/08-1 and should be avoided for cavern placement (Fig. 9).

Implications

This study identifies a number of halite-dominated facies within layered evaporite sequences that would be suitable sites for hydrogen storage in the FAB. Wells confirm that the AHF and upper LHF reach sufficient thickness, depth and halite purity to support safe and effective salt solution mining in the basin centre (Fig. 10). The basin margins do not see sufficient halite thickness to provide economic storage sites. Salt diapirs are also a likely candidate for salt mining (Fig. 10); however, targets must be carefully mapped to ensure sufficient burial depth. The FAB provides an excellent opportunity for integrating offshore wind with offshore hydrogen generation and salt cavern storage, where surface infrastructure works in harmony with the subsurface geology (Fig. 10).

The FAB is one of many salt basins found globally. Each basin has its own unique precipitation history, resulting in a unique stratigraphy of interbedded halites, potassium salts, anhydrites, carbonates and clastics (Jackson and Hudec 2017; Rowan *et al.* 2019). These different precipitation histories present unique challenges in de-risking other salt basins for hydrogen storage in salt caverns. This study emphasizes the importance of well data for understanding the suitability of evaporite sequences for cavern mining. In particular, petrophysical data can play an important role in understanding the heterogeneities of halite units that can impact cavern capacity and integrity (Warren 2017). We show that heterogeneities can be mapped regionally across layered evaporite sequences (Fig. 5). Salt structures, although tending to have higher levels of halite purity, are more challenging to de-risk on account of deformation. Hydrogen storage in salt caverns provides a proven safe and reliable energy store (Beutel and Black 2005; Stone *et al.*

2009; Kruck *et al.* 2013). A robust understanding of the geological distribution of halite bodies in the subsurface and their heterogeneities is ultimately required to ensure safe cavern containment, to model the final cavern geometry and assess the store volume, to support well design, and to mitigate against leakage (Warren 2017; Duffy *et al.* 2022; Pichat 2022).

Legacy hydrocarbon wells such as those used in this study provide critical information on the evaporite facies distribution in the subsurface; however, log suites are often incomplete. GR, RHOB, NPHI and DT logs can be used to understand evaporite facies in the Zechstein; however, modern wireline techniques such as spectral gamma ray and pulsed neutron elemental spectroscopy techniques (Bradley *et al.* 2013; Sullivan and Song 2017) would increase our understanding of heterogeneities within the halite units.

Conclusions

The Forth Approaches Basin (FAB) is located off the eastern coast of the UK and is currently undergoing the development of multiple offshore wind farms. This, combined with its favourable geology, make it a potential candidate for the subsurface storage of hydrogen. The Permian Zechstein is a good candidate for solution mining and salt cavern storage, with sizeable halite-dominated salt structures and halite beds at optimal depths below the seabed. The FAB's geological history makes it the optimal site for salt cavern storage in the Central North Sea where much of the Zechstein has been more deeply buried due to Late Jurassic extension. The depth of salt structures and halite heterogeneity are identified as key risks in the basin when evaluating storage potential, and the true extent of heterogeneous bodies remains uncertain due to a lack of well control.

Petrophysical data from five legacy hydrocarbon wells in the FAB reveal information on the suitability of the Permian Zechstein for solution mining for hydrogen storage. Three halite formations are identified and described: the Z2 Stassfurt Halite Formation (SHF); the Z3 Leine Halite Formation (LHF); and the Z4 Aller Halite Formation (AHF). The SHF is typically less than 100 m thick and its composition varies widely across the FAB, making it challenging to de-risk for solution mining. Where layered, the LHF comprises three subunits. Upper and lower halite-dominated units are separated by a potassium salt-dominated unit that can be mapped regionally in the well data where halokinesis has not occurred. Well 26/04-1 penetrated a thick LHF salt diapir that showed no significant units of potassium salts, only minor heterogeneities. The internal structure of salt diapirs remains a key uncertainty in the FAB due to limited data. The AHF is only seen in the centre of the basin and has the highest halite purity of the sequence. Together, the AHF and LHF could be candidates for solution mining, both in layered sequences and in salt diapirs.

This study demonstrates the value of a re-evaluation of legacy hydrocarbon wells and their re-purposing to support the energy transition. We show that halite units and heterogeneities can be correlated across layered evaporite sequences with good accuracy and used as a predictive tool where data are limited. Diapirs and other salt structures are more challenging to de-risk with respect to halite impurities and internal structures. Legacy data are therefore a critical resource for screening the geological and economic feasibility of potential subsurface storage sites.

Acknowledgements The authors would like to thank the North Sea Transition Authority (NSTA) for providing the datasets via the UK National Data Repository (NDR), and Schlumberger for access to their Petrel software. Our thanks also go to Geoff Page for consultation about the petrophysical responses of evaporitic minerals and latest industry developments. We thank the three reviewers and the editor for their comments that have improved the manuscript and prepared it for publication.

Author contributions **REB**: conceptualization (lead), formal analysis (supporting), supervision (lead), visualization (lead), writing – original draft (lead); **LJR**: data curation (supporting), formal analysis (lead), writing – original draft (supporting); **AJH**: supervision (supporting), writing – review & editing (equal); **DW**: validation (lead), writing – review & editing (lead); **TH**: visualization (supporting), writing – review & editing (supporting).

Funding This research received no specific grant from any funding agency in the public, commercial, or not-for-profit sectors.

Competing interests The authors declare that they have no known competing financial interests or personal relationships that could have appeared to influence the work reported in this paper.

Data availability The datasets generated during and/or analysed during the current study are available in the UK National Data Repository: https://ndr.nstauthority.co.uk

References

Allsop, C., Yfantis, G., Passaris, E. and Edlmann, K. 2023. Utilising publicly available datasets for identifying offshore salt strata and developing salt caverns for hydrogen storage. *Geological Society, London, Special Publications*, **528**, 528–2022, https://doi.org/10.1144/SP528-2022-82

Arsenikos, S., Quinn, M., Kimbell, G., Williamson, P., Pharaoh, T., Leslie, G. and Monaghan, A. 2019. Structural development of the Devono-Carboniferous plays of the UK North Sea. *Geological Society, London, Special Publications*, **471**, 65–90, https://doi.org/10.1144/SP471.3

Baraniuk, C. 2021. The global race to produce hydrogen offshore. BBC News, https://www.bbc.co.uk/news/business-55763356 [last accessed 24 April 2023].

Beutel, T. and Black, S. 2005. Salt deposits and gas cavern storage in the UK with a case study of salt exploration from Cheshire. *Oil Gas European Magazine*, **31**, 31–35.

Bossel, U. and Eliasson, B. 2003. *Energy and the Hydrogen Economy*. Alternative Fuels Data Center, Arlington, VT.

Brackenridge, R., Underhill, J.R. and Jamieson, R. 2018. *The Mid North Sea High: Controls on Structure, Stratigraphy and Prospectivity*. Technical report and supporting documentation released by the Oil and Gas Authority UK.

Brackenridge, R.E., Underhill, J.R., Jamieson, R. and Bell, A. 2020. Structural and stratigraphic evolution of the Mid North Sea High region of the UK Continental Shelf. *Petroleum Geoscience*, **26**, 154–173, https://doi.org/10.1144/petgeo2019-076

Bradley, T.J., Mendez, F., Longo, J., Bullen, J. and Visser, J. 2013. Application of pulsed neutron mineralogy tools to the evaluation of evaporite deposits. *In*: 75th EAGE Conference & Exhibition incorporating SPE EUROPEC, 10–13 June 2013. European Association of Geoscientists & Engineers (EAGE), Houten, The Netherlands, https://doi.org/10.3997/2214-4609.20130799

Caglayan, D.G., Weber, N., Heinrichs, H.U., Linßen, J., Robinius, M., Kukla, P.A. and Stolten, D. 2020. Technical potential of salt caverns for hydrogen storage in Europe. *International Journal of Hydrogen Energy*, **45**, 6793–6805, https://doi.org/10.1016/j.ijhydene.2019.12.161

Cameron, T.D.J. 1993. 5. Carboniferous and Devonian of the Southern North Sea. *In:* Knox, R.W.O'B. and Cordey, W.G. (eds) *Lithostratigraphic Nomenclature of the UK North Sea*. British Geological Survey, Keyworth, Nottingham, UK.

Cartwright, J., Stewart, S. and Clark, J. 2001. Salt dissolution and salt-related deformation of the Forth Approaches Basin, UK North Sea. *Marine and Petroleum Geology*, **18**, 757–779, https://doi.org/10.1016/S0264-8172(01)00019-8

Clark, J.A., Stewart, S.A. and Cartwright, J.A. 1998. Evolution of the NW margin of the North Permian Basin, UK North Sea. *Journal of the Geological Society, London*, **155**, 663–676, https://doi.org/10.1144/gsjgs.155.4.0663

Clave, C.M., Simonin, A.O., Marshal, A.M. and Vandeginste, V. 2019. Impact of impurities in salt rock for underground gas storage in salt caverns. *Geophysical Research Abstracts*, **21**, EGU2019-16684-2, https://meetingorganizer.copernicus.org/EGU2019/EGU2019-16684-2.pdf

Cluff Oil 1986. *Forth Approaches Basin, UK North Sea Continental Shelf Final Well Report 26/12-1*. Report 08/86. Cluff Oil plc, London.

Crain, E.R. 2014. Potash Petrophysics – Then and now. CSPG Reservoir, 07 20-25, September, https://www.spec2000.net/freepubs/2014-5%20Potash%20Petrophysic%20-%20Then%20and%20Now%20CSPG%20Crain.pdf [last accessed 1 August 2022].

Crotogino, F. 2022. Large-scale hydrogen storage. *In*: Letcher, T.M. (ed.) *Storing Energy with Special Reference to Renewable Energy Sources*. 2nd edn. Elsevier, Amsterdam, 613–632, https://doi.org/10.1016/B978-0-12-824510-1.00003-9

Crotogino, F., Donadei, S., Bünger, U. and Landinger, H. 2010. Large-scale hydrogen underground storage for securing future energy supplies. *In:* Stolten, D. and Grube, T. (eds) *Proceedings of the 18th World Hydrogen Energy Conference 2010 – WHEC 2010. Parallel Sessions Book 4: Storage Systems/*

Policy Perspectives, Initiatives and Co-operations. Forschungszentrum Jülich, Jülich, Germany, 61–70.

Doornenbal, H. and Stevenson, A. 2010. *Petroleum Geological Atlas of the South Permian Basin Area*. European Association of Geoscientists & Engineers (EAGE), Houten, The Netherlands.

Duffy, O.B., Hudec, M. *et al.* 2022. The role of salt tectonics in the energy transition: an overview and future challenges. *Earth ArXiv*, https://doi.org/10.31223/X5363J

Element Energy 2020. *Aberdeen Hydrogen Hub: Vision and Business Case for Establishing Scalable Renewable Hydrogen Supplies in the City*. Aberdeen Hydrogen Hub Executive Summary, https://northsearegion.eu/media/17360/acc-hydrogen-hub-business-case.pdf [last accessed 12 August 2022].

Erratt, D., Thomas, G. and Wall, G. 1999. The evolution of the Central North Sea Rift. *Geological Society, London, Petroleum Geology Conference Series*, **5**, 63–82, https://doi.org/10.1144/0050063

Evans, D.J. and Holloway, S. 2009. A review of onshore UK salt deposits and their potential for underground gas storage. *Geological Society, London, Special Publications*, **313**, 39–80, https://doi.org/10.1144/SP313.5

Fisher, M.J. and Mudge, D.C. 1990. Triassic. *In:*Glennie, K.W. (ed.) *Introduction to the Petroleum Geology of the North Sea*. Blackwell, Oxford, UK, 191–218.

Franklin, M., Fraenkel, P., Yendell, C. and Apps, R. 2022. Gravity energy storage systems. *In*: Letcher, T.M. (ed.) *Storing Energy with Special Reference to Renewable Energy Sources*. 2nd edn. Elsevier, Amsterdam, 91–116.

Gahleitner, G. 2013. Hydrogen from renewable electricity: an international review of power-to-gas pilot plants for stationary applications. *International Journal of Hydrogen Energy*, **38**, 2039–2061, https://doi.org/10.1016/j.ijhydene.2012.12.010

Gearhart Geodata Services 1984. *End of Well Report for Tricentrol Well Number 26/14-1*. Report R3240913. Gearhart Geodata Services Ltd, Aberdeen, UK.

Glenister, I., Milner, S., Jones, B. and Elsinger, B. 2002. *26/4-1 Well Resume: License P.0987*. Report ER02008. Shell UK Ltd, London.

Glennie, K.W. and Underhill, J.R. 1998. Origin, development and evolution of structural styles. *In:* Glennie, K.W. (ed.) *Petroleum Geology of the North Sea: Basic Concepts and Recent Advances*. 4th edn. Blackwell Science, Oxford, UK, 42–84.

Goldsmith, P.J., Rich B. and Standring, J. 1995. Triassic correlation and stratigraphy in the south Central Graben, UK North Sea. *Geological Society, London, Special Publications*, **91**, 123–143, https://doi.org/10.1144/GSL.SP.1995.091.01.07

Heinemann, N., Booth, M.G., Haszeldine, R.S., Wilkinson, M., Scafidi, J. and Edlmann, K. 2018. Hydrogen storage in porous geological formations – onshore play opportunities in the Midland Valley (Scotland, UK). *International Journal of Hydrogen Energy*, **43**, 20 861–20 874, https://doi.org/10.1016/j.ijhydene.2018.09.149

HM Government 2021. *UK Hydrogen Strategy*. CP 475. Presented to Parliament by the Secretary of State for Business, Energy & Industrial Strategy by Command of Her Majesty. APS Group on behalf of the Controller of Her Majesty's Stationery Office, https://assets.publishing.service.gov.uk/government/uploads/system/uploads/attachment_data/file/1011283/UK-Hydrogen-Strategy_web.pdf

Jackson, M. and Hudec, M. 2017. *Salt Tectonics: Principles and Practice*. Cambridge University Press, Cambridge, UK, https://doi.org/10.1017/9781139003988

Johnson, H., Warrington, G. and Stoker, S.J. 1993. 6. Permian and Triassic of the Southern North Sea. *In:*Knox, R.W.O'B. and Cordey, W.G. (eds) *Lithostratigraphic Nomenclature of the UK North Sea*. British Geological Survey, Keyworth, Nottingham, UK.

Kearsey, T.I., Millward, D., Ellen, R., Whitbread, K. and Monaghan, A.A. 2019. Revised stratigraphic framework of pre-Westphalian Carboniferous petroleum system elements from the Outer Moray Firth to the Silverpit Basin, North Sea, UK. *Geological Society, London, Special Publications*, **471**, 91–113, https://doi.org/10.1144/SP471.11

Kruck, O., Crotogino, F., Prelicz, R. and Rudolph, T. 2013. *Assessment of the Potential, the Actors and Relevant Business Cases for Large Scale and Seasonal Storage of Renewable Electricity by Hydrogen Underground Storage in Europe*. Deliverable No. 3.1. HyUnder Project, https://hyunder.eu/wp-content/uploads/2016/01/D3.1_Overview-of-all-known-underground-storage-technologies.pdf [last accessed 12 August 2022].

Lysyy, M., Fernø, M. and Ersland, G. 2021. Seasonal hydrogen storage in a depleted oil and gas field. *International Journal of Hydrogen Energy*, **46**, 25 160–25 174, https://doi.org/10.1016/j.ijhydene.2021.05.030

McKellar, Z., Hartley, A.J., Morton, A.C. and Frei, D. 2020. A multidisciplinary approach to sediment provenance analysis of the late Silurian–Devonian Lower Old Red Sandstone succession, northern Midland Valley Basin, Scotland. *Journal of the Geological Society, London*, **177**, 297–314, https://doi.org/10.1144/jgs2019-063

Michalski, J., Bünger, U. *et al.* 2017. Hydrogen generation by electrolysis and storage in salt caverns: potentials, economics and systems aspects with regard to the German energy transition. *International Journal of Hydrogen Energy*, **42**, 13 427–13 443, https://doi.org/10.1016/j.ijhydene.2017.02.102

Mobil 1992. *26/8-1 Formation Evaluation Log*. Exlog. Mobil Corporation, Fairfax, VA.

Mobil North Sea 1993. *Geological Final Well Report Well 26/8-1*. Exploration Operations May 1993. Mobil North Sea Ltd, Aberdeen, UK.

Muhammed, N.S., Haq, B., Al Shehri, D., Al-Ahmed, A., Rahman, M.M. and Zaman, E. 2022. A review on underground hydrogen storage: insight into geological sites, influencing factors and future outlook. *Energy Reports*, **8**, 461–499, https://doi.org/10.1016/j.egyr.2021.12.002

Neville, R.S.W. and Wreglesworth, I. 1984. *Tricentrol 26/14-1 British North Sea Well: Biostratigraphy of the Interval 1400′–4127′ TD*. Report 3126P/A. Robertson Research International Ltd, Crawley, UK.

Pichat, A. 2022. Stratigraphy, paleogeography and depositional setting of the K–Mg salts in the Zechstein Group of Netherlands – implications for the development of salt caverns. *Minerals*, **12**, 486, https://doi.org/10.3390/min12040486

Rowan, M.G., Urai, J.L., Fiduk, J.C. and Kukla, P.A. 2019. Deformation of intrasalt competent layers in different modes of salt tectonics. *Solid Earth*, **10**, 987–1013, https://doi.org/10.5194/se-10-987-2019

Sarajlic, M., Takach, M. *et al.* 2021. Utilizing underground caverns as energy storage for future energy systems: challenges for grid integration. Presented at the CIGRE International Symposium, 21–24 November 2021, Ljubljana, Slovenia.

Seagreen Wind Energy 2014. Marine Scotland consents Firth of Forth Offshore Wind Phase 1. Seagreen Wind Energy Ltd, Glasgow, UK, https://www.seagreenwindenergy.com/post/marine-scotland-consents-firth-of-for th-offshore-wind-phase-1 [last accessed 28 April 2023].

Smith, D.B. 1989. The Late Permian palaeogeography of north-east England. *Proceedings of the Yorkshire Geological Society*, **47**, 285–312, https://doi.org/10.1144/pygs.47.4.285

Smith, N., Evans, D. and Andrews, I. 2005. *The Geology of Gas Storage in Offshore Salt Caverns*. Marine, Coastal and Hydrocarbons Programme. British Geological Survey, Keyworth, Nottingham, UK.

Stephenson, M.H., Ringrose, P., Geiger, S., Bridden, M. and Schofield, D. 2019. Geoscience and decarbonization: current status and future directions. *Petroleum Geoscience*, **25**, 501–508, https://doi.org/10.1144/petgeo2019-084

Stone, H.B., Veldhuis, I. and Richardson, R.N. 2009. Underground hydrogen storage in the UK. *Geological Society, London, Special Publications*, **313**, 217–226, https://doi.org/10.1144/SP313.13

Sullivan, M. and Song, L. 2017. Briggs colour cubing of spectral gamma ray – a novel technique for easier stratigraphic correlation and rock typing. Paper SPWLA-2017-U presented at the SPWLA 58th Annual Logging Symposium, 17–21 June 2017, Oklahoma City, Oklahoma, USA.

Tarkowski, R. 2019. Underground hydrogen storage: characteristics and prospects. *Renewable and Sustainable Energy Reviews*, **105**, 86–95, https://doi.org/10.1016/j.rser.2019.01.051

Tractebel Engie 2021. World's first offshore hydrogen storage concept developed by Tractabel and partners. Tractebel Engie, Brussels, https://tractebel-engie.com/en/news/2021/world-s-first-offshore-hydrogen-storage- concept-developed-by-tractebel-and-partners [last accessed 19 May 2022].

Tucker, M.E. 1991. Sequence stratigraphy of carbonate–evaporite basins: models and application to the Upper Permian (Zechstein) of northeast England and adjoining North Sea. *Journal of the Geological Society, London*, **148**, 1019–1036, https://doi.org/10.1144/gsjgs.148.6.1019

Van Adrichem-Boogaert, H.A. and Kouwe, W.F.P. 1994. *Stratigraphic Nomenclature of the Netherlands; Revision and Update by RGD and NOGEPA*. Verhandelingen van het Koninklijk Nederlands Geologisch Mijnbouwkundig Genootschap, **32**.

Van den Belt, F.J.G. and De Boer, P.I. 2014. An intra-basinal mechanism for marine-evaporite cyclicity. *Journal of the Geological Society, London*, **171**, 461–464, https://doi.org/10.1144/jgs2013-062

Wang, T., Yang, C., Ma, H., Daemen, J.J.K. and Wu, H. 2015. Safety evaluation of gas storage caverns located close to a tectonic fault. *Journal of Natural Gas Science and Engineering*, **23**, 281–293, https://doi.org/10.1016/j.jngse.2015.02.005

Warren, J.K. 2016. Solution mining and salt cavern usage. *In*: *Evaporites*. Springer, Cham, Switzerland, 1303–1374, https://doi.org/10.1007/978-3-319-13512-0_13

Warren, J.K. 2017. Salt usually seals, but sometimes leaks: implications for mine and cavern stabilities in the short and long term. *Earth-Science Reviews*, **165**, 302–341, https://doi.org/10.1016/j.earscirev.2016.11.008

Wiggin, P. 1985. *BP 26/7-1 Geological Well Report*. British Petroleum Development Ltd Exploration and Production Document 143971. British Petroleum Ltd, Sunbury-on-Thames, UK.

Williams, J.D., Williamson, J.P. *et al.* 2022. Does the United Kingdom have sufficient geological storage capacity to support a hydrogen economy? Estimating the salt cavern storage potential of bedded halite formations. *Journal of Energy Storage*, **53**, 105–109, https://doi.org/10.1016/j.est.2022.105109

Zivar, D., Kumar, S. and Foroozesh, J. 2021. Underground hydrogen storage: a comprehensive review. *International Journal of Hydrogen Energy*, **46**, 23 436–23 462, https://doi.org/10.1016/j.ijhydene.2020.08.138